NEW TOOLS IN THE SEARCH FOR SUPERSYMMETRY

A Dissertation

Presented to the Faculty of the Graduate School

of Cornell University

in Partial Fulfillment of the Requirements for the Degree of

Doctor of Philosophy

by

Michael Jinnxien Saelim

August 2014

NEW TOOLS IN THE SEARCH FOR SUPERSYMMETRY

Michael Jinnxien Saelim, Ph.D.

Cornell University 2014

ABSTRACT

The Large Hadron Collider has thrust humanity into the TeV-scale era of particle physics, and with it we have discovered a new Higgs-like particle and set stronger limits on possible theories of supersymmetry and beyond-the-Standard-Model physics. But while the experimental community continues to improve their searches for new physics, the lack of clear beyond-the-Standard-Model discoveries so far has made it apparent that if we are to discover new physics there, the theoretical community must continually develop new methods as well. New tools must be forged and applied to the problems we face at the Large Hadron Collider and possible future particle colliders. This dissertation expresses one contribution, out of many, in this regard.

We begin by using boosted top tagging to look for signals of R-parity conserving supersymmetry. Then we use other jet substructure techniques to look for signals of R-parity violating supersymmetry. Lastly, we use the SUSY-Yukawa sum rule to look beyond the phenomenology and probe the crucial cancellation of divergences at the heart of supersymmetric theories.

BIOGRAPHICAL SKETCH

Michael Saelim was born on a cold Chicago morning to Sou-Ling Chong and Steven Saelim, who instilled in him a great love of learning. He progressed quickly through grade school with a strong affinity for math and science, even pulling his father's algebra textbook off the shelf and reading it cover-to-cover when the school ran out of math for him to study. At Maine South High School, skilled teachers further fed his scientific interests, but nothing held his attention as much as Mr. Downing's and Mr. Marino's physics classes. They, along with fascinating articles in *Scientific American*, inspired him to pursue further study in particle physics.

He then went to Michigan State University, graduating with high honor with dual Bachelor's degrees in physics and mathematics. Along the way, he spent semesters researching at the National Superconducting Cyclotron Laboratory for Dr. Tsang and researching theoretical particle physics for Dr. Repko, and summers exploring other areas of physics with REUs at Indiana University, Los Alamos National Laboratory, and CERN. These days were filled with nerdy friends, losing one's voice at college football and basketball games, the best ice cream ever, and biking through blizzards.

At Cornell University, he pursued a Ph.D. under Dr. Perelstein, researching topics in supersymmetry and collider phenomenology. In his role as a teaching assistant, he had the pleasure to teach hundreds of bright Cornell undergraduate scientists and engineers. Between trivia nights, Scotch Fridays, placing reservations at restaurants for twenty people, and more, he was also blessed to be surrounded by more great friends than he could ever have hoped for.

After receiving his Ph.D., he will return to Chicago to begin a career in software engineering.

To my teachers, who gave the universe structure,
and to my friends and family, who gave the universe meaning.

ACKNOWLEDGEMENTS

Over the past six years, so many people have contributed directly and indirectly to the completion of this Ph.D. — I am forever grateful ...

... first to my advisor, Maxim Perelstein, for giving me the chance to conduct research in particle theory, and for giving me the preparation and guidance I needed so that we could see that research through. I could not have asked for a better mentor.

... to my parents, who have always supported me in everything I try, and who deserve to know, that I know, that I can always rely on them.

... to Csaba, Yuval, Liam, Henry, Jim, Ritchie, Lawrence, Julia, Anders, and Peter, for their invaluable instruction in particle physics, and for fostering a special environment where great particle physics research is done.

... to Josh, Flip, and Andy, for trudging through the grunt work with me, and for passing down the wisdom of the older grad student.

... to Gala, Jordan, Luke, Werner, Frank Wuerthwein, and Didar Dobur, for all their help in understanding the CMS experiment and its ingenious analyses.

... to Katerina, Liz, Kacey, Deb, Cindee, Aimee, Rosemary, Monica, and Peggy, for their administrative expertise and diligence, and for how much they care about everyone in the department.

... to all the other particle theory and experiment postdocs and grad students who have overlapped with me — Avi, Ben Heidenreich, Ben Kreis, Bibhushan, Brando, Brian, Cody, Dan, David Curtin, David Marsh, Dean, Don, Enrico, Gang, Itay, Jack, Javi, Jeff, Jen, Johannes, John, Jolyon, Jorge, Justin, Marco, Mario, Mathieu, Mike, Monika, Naresh, Nathan, Nic Eggert, Nic Rey-Le Lorier, Paul, Riccardo, Robin, Shamayita, Shao Min, Sina, Sohang, Steven, Susan, Thomas, Timm, Walter, Wee-Hao, Xin, Yang, Yao, and Yuhsin — for being the best colleagues and peers.

... to over six incoming classes of graduate students (as well as a few undergraduates)

from the physics, AEP, and other departments — too many to name here — who have been the closest of friends and the craftiest of co-conspirators. They are more important than they know.

TABLE OF CONTENTS

CHAPTER 1

INTRODUCTION

Speaking in the most grandiose terms, the job of a theoretical particle physicist is to build the theoretical framework that encapsulates and explains the structure and nature of the universe. This is the task delegated to us by humanity, because to search for an explanation of what everything is made of and how it all got this way is simply nothing less than our birthright, and our responsibility, as a sentient species.

We stand today on the shoulders of the scientists who came before us: hundreds of years of work have provided us with the Standard Model, an elegant framework that almost everything humanity has observed can be reduced to at small scales. Yet we also look up and see how far we have to go: hundreds more years of work to be spent discovering new physics at even smaller scales, at least until we can reconcile issues with the compatibility of quantum mechanics and general relativity. We consider that perhaps other species in the universe have enjoyed the fruits of this knowledge for many eons, and we envy them, although perhaps they are jealous that we have so many exciting things still to discover.*

*Perhaps that is why they have not contacted us: spoilers.

1.1 Old problems

1.1.1 The Standard Model, and its issues

The current understanding of particle physics is summed up in the Standard Model (SM), which has been built over the last hundred years or so. Gauge fields corresponding to a $SU(3)_C \times SU(2)_L \times U(1)_Y$ symmetry are joined by three generations of fermionic quark and lepton fields, which lie in representations of the Lie algebra. A scalar Higgs field completes the picture by attaining a nonzero vacuum expectation value (vev) that both breaks the $SU(2)_L \times U(1)_Y$ symmetry (in a phenomenon known as electroweak symmetry breaking (EWSB)) and couples to the fermions through Yukawa interactions, giving them mass. In the end, this produces four gauge bosons (a massless photon γ for electromagnetism, massive W and Z bosons for weak interactions, and a massless gluon g for strong interactions), six massive quarks (u, d, c, s, t, b), six massive leptons (e, μ, τ, ν_e, ν_μ, ν_τ), and a single massive Higgs boson h, which was recently discovered at the Large Hadron Collider (LHC).

The SM yields predictions that agree to astounding accuracy with measurements at colliders and other experiments, perhaps the most famous of these being the electron anomalous magnetic dipole moment ($g-2$) which features an agreement to over ten decimal places. But for all its predictive power, the SM still has some faults, chiefly among these being the hierarchy problem. The Higgs boson's two-point function admits a diagram where the Higgs splits into a top quark-antiquark pair, which recombines to reform the Higgs. This top loop diagram introduces a disastrous quadratic divergence to the Higgs mass — if this divergence gets cut off at the high UV scale where new physics is expected (presumably the Planck scale where gravity is expected to enter), it must get

cancelled by a similarly high bare Higgs mass to yield the very small weak-scale physical mass that is observed. This is a troubling example of fine-tuning, where two very large masses must almost perfectly cancel by coincidence. The quest for a natural reason for this sort of cancellation would lead physicists to supersymmetry.

1.1.2 Supersymmetry, and *its* issues

Supersymmetry solves the hierarchy problem in a seemingly drastic manner: fields come in supermultiplets, so that every fermion has an otherwise identical bosonic superpartner, and every boson has an otherwise identical fermionic superpartner. The most minimal version of supersymmetry, known as the Minimal Supersymmetric Standard Model (MSSM), assigns each fermionic quark and lepton a scalar squark or slepton superpartner, and assigns each gauge boson a gaugino fermionic superpartner. In order to properly implement EWSB, the Higgs sector is expanded to generate five Higgs bosons, the lightest of which is expected to be identified with the Higgs boson already discovered. In these supersymmetric theories, the quadratic divergence from the top loop is automatically cancelled by a quadratic divergence of the same magnitude but opposite sign from diagrams with stop loops, elegantly solving the hierarchy problem.

As usual, solving a problem creates new ones. SUSY admits terms in the Lagrangian that violate lepton number (L) conservation and baryon number (B) conservation, which can lead to catastrophes like decaying protons. The most popular way to prevent proton decay is to assume the existence of an extra property known as R-parity, where SM particles have even R-parity and new SUSY particles have odd R-parity. If R-parity is a conserved quantity, these L- and B-violating terms are automatically forbidden. Furthermore, R-parity conservation also implies that there is a lightest SUSY particle (LSP) that

is stable, which may be able to explain the composition of dark matter. Such SUSY models are known as R-parity conserving (RPC) theories. However, there are many models that relax this requirement or do away with it altogether — such models are known as R-parity violating (RPV) theories, and include the Minimal Flavor Violation (MFV) theory described by Csáki, Grossman, and Heidenreich in [48].

Then there is the fact that SUSY must be broken at some high scale. None of these proposed superpartners have been found at collider experiments yet, which necessitates that most of them are heavier than their SM counterparts, even though SUSY should mandate that they have identical masses. But if all possible SUSY-breaking terms are included in the Lagrangian, then over 100 new parameters are added to the model — parameters that are theoretically unconstrained and can lead to large CP-violation and flavor changing neutral currents (FCNCs) that conflict with experiment.

Furthermore, throughout the 2011-2012 runs of the LHC at $\sqrt{s} = 7$ and 8 TeV, no positive signals of new SUSY particles have been found, which pushes the bounds on the masses of SUSY particles even higher. As these bounds continue to rise, radiative corrections to the Higgs mass rise as well, leading to fine-tuning, which may defeat the purpose of using SUSY in the first place.

If new SUSY particles are expected at LHC collision energies, where are they? And how can this search be conducted efficiently, when the parameter space is so large? Finally, after finding new particles, can it be shown that they are SUSY superpartners and not new particles of some other theory?

1.2 New tools

1.2.1 Simplified models and motivations for a light third generation

Instead of wrestling with over 100 SUSY parameters, most of the work in collider phenomenology is presented in the framework of simplified models. Simplified models pare down the number of parameters by only considering the minimal set of new particles required to produce the desired SUSY signal. All other SUSY particles are considered either too weakly-coupling or massive to affect the phenomenology, and are decoupled from the system. This has the distinct advantage of paring down the 100+ new SUSY parameters to just a few sparticle masses and assumptions about branching ratios.

One very popular way to search for SUSY is to focus on discovering stops and gluinos, because they are expected to be light and strongly produced at the LHC. Having a stop with greater mass than the top requires SUSY breaking in the stop sector, which disrupts the nice cancellation between the top and stop contributions to the Higgs mass. Letting the stop become much heavier introduces the dominant logarithmic corrections to the Higgs mass at 1-loop order, as in Eq. 1.1. Similarly, since gluino loops contribute to the stop mass, heavy gluinos introduce subdominant logarithmic corrections to the Higgs mass at 2-loop order, as in Eq. 1.2. If these corrections are not so large as to reintroduce fine-tuning, then stops and gluinos must be light and (hopefully) accessible at the LHC [81].

$$\delta m_{H_u}^2\Big|_{\text{stop, LL}} = -\frac{3}{8\pi^2}\, y_t^2\, (m_{Q_3}^2 + m_{u_3}^2 + |A_t|^2)\, \ln\!\left(\frac{\Lambda}{\text{TeV}}\right) \tag{1.1}$$

$$\delta m_{H_u}^2\Big|_{\text{gluino, LL}} = -\frac{2}{\pi^2}\, y_t^2 \left(\frac{\alpha_s}{\pi}\right) |M_3|^2\, \ln^2\!\left(\frac{\Lambda}{\text{TeV}}\right) \tag{1.2}$$

At least one sbottom is also expected to be light, because $\tilde{b}_L$ sits in the same weak isospin

doublet as $\tilde{t}_L$ and thus receives the same SUSY-breaking mass. However, sbottoms are not required to be as light as the stops because the bottom Yukawa is not as strong. Meanwhile, first- and second-generation squarks can still be heavy, with multi-TeV masses. This has the benefit of suppressing FCNCs that haven't been observed in the ample data on processes involving first- and second-generation quarks.

In this work, we will often consider a simplified model pertaining to third-generation SUSY phenomenology at the LHC, consisting of

- the gluino $\tilde{g}$,
- the lightest stop $\tilde{t} \equiv \tilde{t}_1$, and
- if we are considering an R-parity conserving model, the lightest neutralino $\tilde{\chi}^0 \equiv \tilde{\chi}^0_1$.

All other particles are decoupled from the analysis.

1.2.2 Jet substructure and boosted object tagging at the LHC

One of the more exciting recent developments in the search for new particles at the LHC is jet substructure, which results from the production of boosted heavy objects such as high-momentum W and Z bosons, Higgs bosons, and top quarks. If these particles are produced with high p_T and decay hadronically, their decay products may form overlapping jets in the detector. These overlapping jets are seen as a single fat jet, and for a time, it seemed impossible to distinguish these from normal QCD jets.

In 2008, Butterworth, Davis, Rubin, and Salam (BDRS) developed the first boosted object tagger [33], an algorithm that examined the radiation pattern of a jet to discern

whether it was from a boosted heavy object decay or a light quark. Other boosted object taggers followed in the years since [73, 86, 87, 95], but they all work in a similar way: they try to count how many separate lobes, or subjets, there seem to be in the jet's radiation pattern. If there seem to be three, it is likely to be a hadronic top, and if there seem to be two, it is likely to be a W, Z, or h. They also tend to factor in information on the total mass of the jet.

Since their development, jet substructure techniques have begun to be employed at the ATLAS and CMS experiments at the LHC in the search for new particles. The idea is that these new particles must be heavy, and can decay into Ws, Zs, Higgs bosons, and top quarks. If the new particles are much heavier than their decay products, those decay products will end up being boosted heavy objects that will result in fat jets with substructure, and it becomes imperative to distinguish them from normal jets.

In Chapter 2, we discuss a proposed LHC search for light stops and gluinos, in an R-parity conserving SUSY model, that takes advantage of boosted top tagging. We consider a simplified model with a gluino $\tilde{g}$, light stop $\tilde{t}$, and neutralino LSP $\tilde{\chi}^0$, where the gluino is heavier than the stop. In this model, gluinos are pair-produced and decay to on-shell top and on-shell stop, and the stop decays to on-shell top and neutralino:

$$pp \to \tilde{g}\tilde{g} \ , \qquad \begin{cases} \tilde{g} \to t\tilde{t}^* \ , \ \tilde{t}^* \to \bar{t}\tilde{\chi}^0, \\ \tilde{g} \to \bar{t}\tilde{t} \ , \ \tilde{t} \to t\tilde{\chi}^0. \end{cases} \tag{1.3}$$

The production of four on-shell tops motivates us to use top tagging to generate handles on this signal, and we show the statistical power of this analysis with a Monte Carlo study.

In Chapter 3, we discuss a proposed LHC search for light stops and gluinos, in an R-parity violating SUSY model, that takes advantage of jet substructure. We consider a

simplified model motivated by the Minimal Flavor Violation (MFV) model [48] with a gluino $\tilde{g}$ and light stop LSP $\tilde{t}$. In this model, gluinos are pair-produced and decay to top and stop, and the stop decays to b and s quarks, violating R-parity:

$$pp \to \tilde{g}\tilde{g} \ , \qquad \begin{cases} \tilde{g} \to t\tilde{t}^* \ , \ \tilde{t}^* \to bs, \\ \tilde{g} \to \overline{t}\tilde{t} \ , \ \tilde{t} \to \overline{b}\overline{s}. \end{cases} \tag{1.4}$$

If the gluino is much heavier than the stop, the stops become boosted heavy objects, which motivates using jet substructure techniques to identify them. We show the statistical power of this analysis with a Monte Carlo study, which also reveals a surprisingly good performance even for heavy off-shell stops.

1.2.3 The SUSY-Yukawa sum rule

Looking farther ahead into the future, once new particles are discovered at the LHC, can they be shown to come from SUSY? It is possible that other models can generate similar particle content, which necessitates a way to probe the theoretical mechanism behind the stabilization of the Higgs mass. In 2010, Blanke, Curtin, and Perelstein developed the SUSY-Yukawa sum rule [28], which is an algebraic relation between the third-generation squark masses and mixing angles that should hold if SUSY is responsible for the cancellation of quadratic divergences in the Higgs mass. However, while this relation is exact at tree-level, it is subject to radiative corrections that are dependent on the other SUSY parameters in the model.

In Chapter 4, we discuss a proposal to use experimental measurements of the other new particles at the LHC and a future e^+e^- collider to constrain the SUSY parameter space, thus constraining the distribution of possible radiative corrections to the sum rule. This necessarily involves scanning over the SUSY parameter space, but this seems at first

computationally prohibitive. Instead, we use Markov chain Monte Carlo (MCMC) to probe a subset of the phenomenological MSSM (pMSSM) parameter space, and show the feasibility of this sum rule technique.

Finally, Chapter 5 concludes the work of this dissertation, which has been in pursuit of the theoretical framework that encapsulates and explains the structure and nature of the universe.

CHAPTER 2

LOOKING FOR R-PARITY CONSERVING SUSY

Higher collision energies at the LHC motivate the use of top tagging in BSM searches. Decays of new heavy particles can produce top quarks that are highly boosted in the lab frame, collimating the top's hadronic decay products into a single "fat jet" that can be separated from light quark jets by its three-pronged substructure and invariant mass. We focus here on a SUSY search for gluino pair production that results in a final state with up to four boosted tops, which can be tagged and used to identify the SUSY events.

This chapter is based on the paper *Boosted Tops from Gluino Decays* [24], written in collaboration with Joshua Berger, Maxim Perelstein, and Andrew Spray.

2.1 Boosted Tops from Gluino Decays

2.1.1 Introduction

Recently, experiments at the Large Hadron Collider (LHC) have begun searching for new physics beyond the Standard Model (SM). Among the many theoretical ideas about the possible nature of this new physics, supersymmetry (SUSY) is the most popular one: it provides an appealing solution to the gauge hierarchy problem of the SM, contains an attractive dark matter candidate, and fits naturally in the framework of grand unification and string theory. SUSY models predict a number of new particles, "superpartners" of the known SM particles, which may be produced at the LHC. In the simplest SUSY models, all superpartners are odd under a discrete symmetry, R-parity, while all SM particles are R-even. This implies that the lightest SUSY particle (LSP) is stable, and that any other superpartner will decay to the LSP and one or more SM particles. Cosmological considerations strongly prefer the LSP to be electrically neutral and uncolored, so that at the LHC the LSP passes through the detector without interactions, leading to an apparent transverse momentum imbalance, or "missing transverse energy" (MET). The presence of MET provides a distinct signature which can be used to distinguish SUSY events from the (far more numerous) SM backgrounds.

At the time of writing, the LHC experiments have presented searches for events with anomalous MET using a data set of approximately 1 fb^{-1} collected in 2010-11 at the center-of-mass energy of $\sqrt{s} = 7$ TeV. No evidence for anomalous MET has been found, and limits on superpartner masses have been set. Barring accidental features such as spectrum degeneracies, gluinos $\tilde{g}$ and squarks of the first two generations $\tilde{q}_{1,2}$ have been ruled out for masses up to about 1 TeV [4, 39]. In models where all squarks have a common mass

at some energy scale, this bound implies that a significant amount of fine-tuning would be necessary to accommodate the observed electroweak symmetry breaking scale [93]. On the other hand, fine-tuning can be avoided if the third-generation squarks, stops $\tilde{t}$ and sbottoms $\tilde{b}$, are significantly lighter than $\tilde{q}_{1,2}$ [30, 81, 75, 53]. The LHC bounds on third-generation squarks are quite weak: stops above 200-300 GeV are currently allowed. The only other superpartner whose mass is significantly constrained by naturalness is the gluino [30]; at present, gluinos above 600 GeV are allowed if decaying only via the 3rd generation. With this motivation, we will focus on a scenario where gluinos, third-generation squarks, and a neutralino LSP are the only particles relevant for the LHC phenomenology, with other squarks being too heavy to be produced. An explicit example of a complete theory realizing this spectrum is the "accidental SUSY" models [65, 94, 66].

The lack of discovery so far also implies that traditional SUSY searches using the MET signature will become more difficult, since the large-MET tails of SM backgrounds will need to be calculated (or extrapolated) with increasingly high precision to obtain sensitivity to lower SUSY cross sections. This motivates the question: Can any handles other than MET be used to identify SUSY events in the presence of large SM backgrounds? In this section, we explore an alternative signature. Gluino cascade decays to the LSP via intermediate stops produce two top quarks, so that gluino pair-production events may result in final states with four tops [96, 72, 8]. If the gluino-stop and stop-LSP mass differences are sufficiently large, each of these tops will typically be relativistic in the lab frame, and its hadronic decay products will be merged into a single jet. Recently, much work has been done on distinguishing such top jets from the usual hadronic jets using the energy distribution inside the jet, and several well-tested algorithms for "tagging" top jets are now available [5]. The original motivation was to search for decays of the Kaluza-Klein gluon in models with extra dimensions [9, 78]; other proposed applications

include a search for the string-Regge excitation of the gluon [84], and a search for direct stop production in SUSY [87]. Here, we point out that this technique can also be used to search for the SUSY gluino, and is particularly promising in scenarios with a light third generation, since $\tilde{g}$ decays to tops have large branching fractions in this case.

2.1.2 Analysis Setup

In the spirit of the "simplified model" approach [12, 60], we assume that a gluino $\tilde{g}$, one stop $\tilde{t}$, and a single neutralino $\tilde{\chi}^0$ are the only superpartners relevant for the LHC phenomenology. This is the minimal set of particles required to produce our signature. In the Minimal Supersymmetric Standard Model (MSSM), this setup can be realized if the second stop and the left-handed sbottom are heavier than the gluino. (Note that naturalness considerations in the MSSM prefer spectra with a few hundred-GeV splitting among the two stop mass eigenstates [83].) If this is not the case, the branching ratios of the decays producing our signature would be reduced (e.g. from 1 to 2/3 if all three squarks are degenerate), resulting in a somewhat decreased rate, but qualitatively the picture is unchanged. We assume that the neutralino is the stable LSP, and set its mass to 60 GeV throughout the analysis. The LHC signal is dominated by gluino pair-production, followed by the cascade decay

$$\tilde{g} \to \tilde{t} + \bar{t}, \quad \tilde{t} \to t\tilde{\chi}^0, \tag{2.1}$$

or its charge conjugate. We assume that $m_{\tilde{g}} - m_{\tilde{t}} > m_t$, $m_{\tilde{t}} - m_{\tilde{\chi}^0} > m_t$, so that all four tops in the event are on-shell. (It may be possible to relax one of these conditions, as long as the other one is satisfied strongly so that at least two tops in the event are boosted; we will not study that possibility here.) We compute gluino pair-production cross sections at next-to-leading order (NLO) using `PROSPINO` [22]. To study cut efficiencies, we

generate event samples for gluino pair-production followed by the decays (2.1) using MadGraph/MadEvent v5 1.3.27 (MG/ME) [13] for a large set of parameters $(m_{\tilde{g}}, m_{\tilde{t}})$. We then simulate top decays, showering and hadronization with PYTHIA 8 [92]. To identify jets, we use the anti-k_T algorithm implemented in the FastJet code [36, 34, 35]. Top tagging of jets in our sample is simulated using the implementation of the Hopkins algorithm [73] available at [35]. In the top tagger, we use two sets of parameters, "tight" and "loose" tags; they are defined precisely as in [5].

We require at least 4 jets with $p_T > 100$ GeV in each event, and require that some of the jets be top-tagged. (The optimal number of top-tagged jets required depends on the LHC energy and luminosity, see below.) In the signal, tagged jets are typically due to hadronic decays of boosted tops, which produce 3 collimated partons that cannot be resolved. The backgrounds include SM processes with boosted tops, as well as ordinary jets mistakenly tagged as top-jets. (The mistag probability is typically of order 1% [5].) We also require the presence of substantial missing energy. The irreducible backgrounds may contain MET from invisible Z decays, leptonic W decays, or semileptonic top decays. We include the following irreducible backgrounds: $nt + (4-n)j$ with $n = 1 \ldots 4$; $Z + nt + (4-n)j$, with $n = 0, 2, 4$; and $W + nt + (4-n)j$, with $n = 0, 2, 4$. Here each t may be a top or an anti-top, j denotes a jet due to a non-top quark or a gluon, and $Z \to \nu\bar{\nu}$ or $W \to \ell\nu$ is required. We do not include reducible backgrounds, other than the light jets mistagged as tops. We simulated the backgrounds at parton level with MG/ME, and used these samples to compute p_T and MET cut efficiencies. We use leading-order (LO) cross sections for all background processes. The two dominant backgrounds, $2t + 2j$ and $Z + 4j$, have been recently computed at NLO. In both cases, the NLO correction to the cross section is negative: K-factors of 0.73 for $2t + 2j$ [26] and 0.95 for $Z + 4j$ [70] have been reported, so that using LO cross sections for these processes is conservative. No other backgrounds

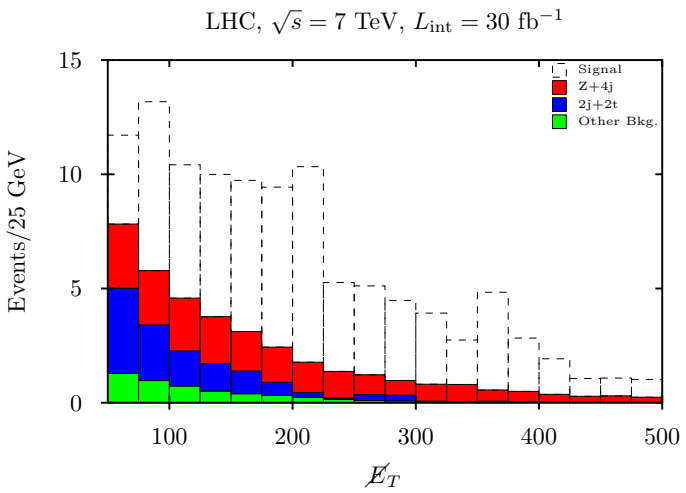

Figure 2.1: Signal at the benchmark point, $(m_{\tilde{g}}, m_{\tilde{t}}) = (800, 400)$ GeV, and background rates as a function of MET, at 7 TeV LHC. Four jets with $p_T > 100$ GeV and two top-tagged jets are required.

are currently known beyond the LO.

Unfortunately, due to large QCD rates and small mistag probabilities, we were not able to generate Monte Carlo samples large enough to measure top-tag efficiencies directly in the background channels. Instead, we estimate these efficiencies by multiplying the p_T-dependent tag and mistag probabilities for individual top and non-top jets reported in Ref. [5]. This estimate assumes that the tag and mistag probabilities for each jet are independent of the presence of other objects in the final state (the probabilities in [5] were computed using $t\bar{t}$ and $2j$ samples). The probability to tag a true top jet as such is clearly reduced by the presence of other jets in the event: for example, the tag efficiency for our signal approximated in this way is typically about a factor of two higher than that obtained by a full simulation. So, our estimate of backgrounds involving tops, such as $2t + 2j$, is certainly conservative. It is less clear how the mis-tag probability would be affected; we leave this issue for future work.

2.1.3 LHC Sensitivity at $\sqrt{s} = 7$ TeV

To keep the analysis simple, we optimize the selection cuts for a single "benchmark" point in the model parameter space, and do not vary them as we scan the masses. At 7 TeV, we choose the benchmark point $(m_{\tilde{g}}, m_{\tilde{t}}) = (800, 400)$ GeV. We studied all possible combinations of between 0 and 4 loose and tight top tags, and conclude that requiring 2 loose tags is the best strategy at this point. Analyses requiring more than 2 tags, or 2 or more tight tags, suffer from low event rate, making a search in the 7 TeV LHC run with $20 - 30$ fb^{-1} integrated luminosity impractical. Requiring fewer tags leads to significantly higher background rates, decreasing sensitivity [18].

The two top tag requirements strongly suppress the backgrounds, as illustrated in Table 2.1, but are not by themselves sufficient, so that an additional MET cut must be applied. The signal and principal backgrounds as a function of MET are shown in Fig. 2.1. We require $\not{E}_T > 100$ GeV; with this cut, we expect 32 signal events, $S/B = 2.4$, and statistical significance of 6.8 at the benchmark point with 30 fb^{-1} integrated luminosity. The reach of the LHC with this data set is shown in Fig. 2.2. (The 95% exclusion contour is calculated using the expected CL_s [71, 88]. The discovery significance is determined using the expected log likelihood of consistency with the signal plus background hypothesis [62, 20].) Gluino masses of up to about 1 TeV can be probed at the 95% confidence level, as long as the gluino-stop mass difference exceeds 400 GeV. The 5-sigma discovery reach extends to a gluino mass of about 900 GeV for stop masses below 350 GeV. We should also note that $S/B \gtrsim 1$ throughout the probed region, so no extraordinarily precise predictions of the background are required.

Process	$\sigma_{\rm tot}$	Eff(p_T)	Eff(tag)	$\sigma_{\rm tag}$	Eff($\not{E}_T$)	$\sigma_{\rm all\ cuts}$
signal	61.5	37	6	1.31	81	1.06
$Z+4j$	2×10^5	0.2	0.1	0.44	66	0.29
$2t+2j$	5×10^4	3	0.3	5.7	2	0.10
$W+4j$	2×10^5	0.2	0.03	0.12	29	0.04
$Z+2t+2j$	50	4	1	0.02	72	0.02

Table 2.1: Signal and background cross sections (in fb) and cut efficiencies (in %) at the 7 TeV LHC. Acceptance cuts of $p_T > 20$ GeV, $|\eta| < 5$ for all jets are included in the total cross sections. The cuts are labelled as follows: "p_T": requiring 4 jets with $p_T > 100$ GeV; "tag": requiring 2 jets to be tagged as tops with "loose" parameters; "$\not{E}_T$": requiring $\not{E}_T > 100$ GeV. The signal is at the benchmark point, $(m_{\tilde{g}}, m_{\tilde{t}}) = (800, 400)$ GeV. Backgrounds not listed here are negligible.

2.1.4 LHC Sensitivity at $\sqrt{s} = 14$ TeV

Anticipating higher reach of the search at 14 TeV, we optimize the selection cuts for a benchmark point with higher masses, $(m_{\tilde{g}}, m_{\tilde{t}}) = (1200, 600)$ GeV. After again considering all possible combinations of loose and tight tag requirements, we conclude that the optimal strategy in this case is to require three loose tags. We further require $\not{E}_T \geq 175$ GeV. At the benchmark point, we expect 8.5 signal events to pass these cuts in a data set of 10 fb^{-1}, and with $S/B = 27.5$ the expected statistical significance of observation is 6.5. The reach of a search with these parameters is shown in Fig. 2.3. Discovery is possible up to $1.3 - 1.4$ TeV gluino masses with stops in the $300 - 700$ GeV mass range. In this case, $S/B \gtrsim 10$ throughout the discovery region.

Given how effective the top tagging technique is in suppressing backgrounds, it is natural to wonder whether, given enough data, a search for gluinos could be conducted with no MET requirement at all. Unfortunately, this is not possible. While the backgrounds studied above are sufficiently suppressed, a new irreducible background, pure QCD events with 4 hard jets ($p_T > 100$ GeV), must be included in the absence of a MET cut. The rate for this process is so large (5.3 nb at 14 TeV at tree-level) that, even including

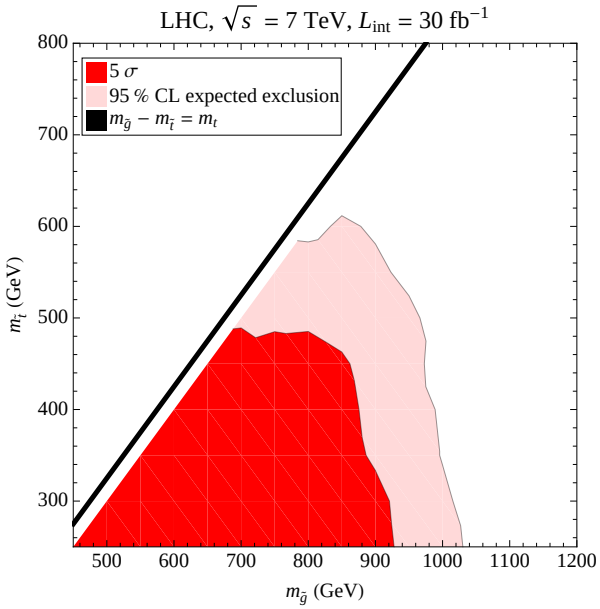

Figure 2.2: The 95% c.l. expected exclusion and 5-sigma discovery reach of the proposed search at the 7 TeV LHC run with 30 fb^{-1} integrated luminosity.

the small mistag probabilities for light jets, it overwhelms the signal. We estimate that the most sensitive search without a MET cut is again one with 3 loose top tags required. For a 300 fb^{-1} data set, this search is sensitive to the benchmark point at about 4.5 sigma level (statistics-only), but with $S/B \sim 0.1$, systematic errors are probably too large to claim sensitivity.

2.1.5 Discussion

Our analysis indicates that using tagged top jets as an additional handle to suppress SM backgrounds in the search for gluino decaying to stops leads to interesting reach, even in the 7 TeV run. In fact, the reach may be even higher than we estimate, since we did not perform a thorough cut optimization for various regions of the model parameter space, instead simply freezing the cuts to values that were found to be near-optimal for a single

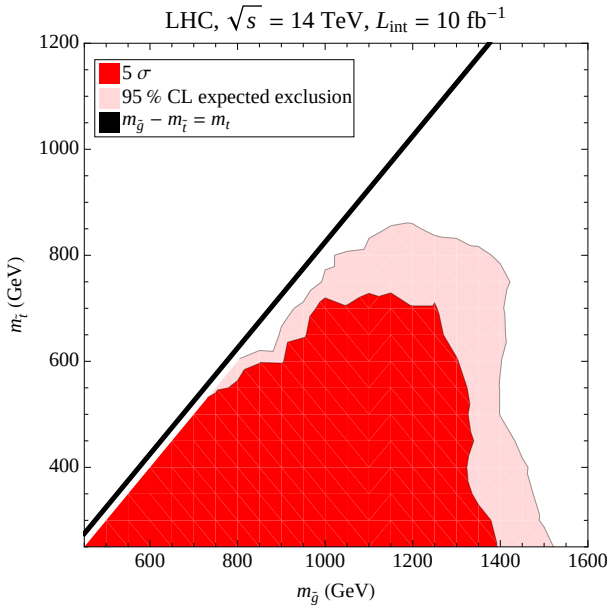

Figure 2.3: The 95% c.l. expected exclusion and 5-sigma discovery reach of the proposed search at the 14 TeV LHC run with 10 fb^{-1} integrated luminosity.

benchmark point.

While we made several simplifications in this exploratory study, the promising results in our opinion justify a more complete analysis. Most of the outstanding issues concern backgrounds. For irreducible backgrounds, the fixed-order (tree-level) simulations used here should be supplemented with showering and hadronization, although since the jets used in our analysis are required to have rather high p_T, we do not expect qualitative changes. Also, MC samples with higher statistics should be used to fully simulate top-tagging efficiencies on the backgrounds. Reducible backgrounds, which were ignored here, should be studied. The most important one of these is the pure QCD channel, $4j$ at parton level, which has a very high rate even with a 2 or 3 mistagged-jet requirement. The pure-QCD events passing our cuts lie far on the tail of the MET distribution for this channel, where the MET is entirely due to undetected or incorrectly measured jets. Correctly estimating this background would thus be a task for a complete detector simulation or a

data-driven approach, which must be performed by the experimental collaborations. It is important to note, however, that large-MET QCD tails affect all SUSY searches at the LHC relying on MET, and in the purely hadronic searches this effect is typically subdominant to the reducible backgrounds once appropriate cuts are applied to eliminate events with MET aligned with one of the jets [4, 39]. Similar techniques can be applied in our case.

2.1.6 Conclusions

If SUSY is realized in such a way that stops and sbottoms are the only squarks below the TeV scale, as favored by naturalness and recent negative results from the LHC, top-rich final states are a natural place to search for it. Our results indicate that the techniques to separate top jets from light jets, developed recently with a completely different motivation, can be employed to boost sensitivity of such searches. They can complement other proposed strategies for this scenario [72, 8, 29], especially in the heavy gluino region. We encourage the experimental collaborations to incorporate this tool in the upcoming searches.

CHAPTER 3

LOOKING FOR R-PARITY VIOLATING SUSY

The lack of SUSY discoveries at the LHC so far challenges the assumption of R-parity conservation, which predicts that the lightest SUSY particles should be stable and neutral, generating significant missing transverse energy (MET) in SUSY events. While RPV SUSY signals are more challenging to find without being able to rely on MET, signals with same-sign dilepton (SSDL) signatures remain promising because of their extremely low SM background. We focus here on a search for gluino pair production where intermediate stops RPV-decay to two down-type quarks, which can lead to a SSDL signature with b-jets and very little MET. We recast a recent search by the CMS experiment for this signature, and we propose improvements to the search for RPV SUSY that take advantage of large jet masses and jet substructure algorithms such as N-subjettiness.

This chapter is based on the paper *The Same-Sign Dilepton Signature of RPV/MFV SUSY* [25], written in collaboration with Joshua Berger, Maxim Perelstein, and Flip Tanedo, as well as the follow-up paper *RPV SUSY with Same-Sign Dileptons at LHC-14* [90], written in collaboration with Maxim Perelstein and contributed to the Snowmass Community Summer Study 2013.

3.1 The Same-Sign Dilepton Signature of RPV/MFV SUSY

3.1.1 Introduction

Supersymmetry (SUSY) remains one of the most compelling ideas for extending the Standard Model (SM). While SUSY is clearly broken in nature, naturalness of electroweak symmetry breaking strongly suggests that it should be restored at an energy scale $\lesssim 1$ TeV. This would require the SUSY partners of the SM particles to appear at that scale. However, experiments conducted in 2010–2012 at the Large Hadron Collider (LHC) have seen no evidence for such superpartners, placing lower bounds on the masses of some of them, squarks and gluinos, well in excess of 1 TeV. This apparent contradiction led many theorists to question the assumptions underlying the LHC searches. One of the most important assumptions is R-parity conservation, which implies that the lightest superpartner (LSP) is stable. A stable LSP in turn implies that each event with superpartner production contains either missing transverse energy (MET) or exotic charged tracks, either of which provides a good handle to distinguish such events from the SM backgrounds. Most LHC searches make extensive use of such handles. If there is no conserved R-parity, these searches would not be applicable and the LHC bounds would be weakened significantly, removing conflict with naturalness.

From the theoretical point of view, R-parity is *not* required by SUSY: it is an additional discrete symmetry. The motivation for introducing this extra symmetry is purely phenomenological: it forbids baryon (B) and lepton (L) number violating operators that would otherwise induce rapid proton decay. However, proton decay and other tightly constrained B- and L-violating processes may be forbidden or suppressed to acceptable levels *without* introducing R-parity. An interesting proposal along these lines has been

made recently by Csaki, Grossman and Heidenreich [48] (see also [80]). The authors start with a minimal SUSY model without R-parity. They then impose the Minimal Flavor Violation (MFV) hypothesis, which is strongly motivated by flavor physics constraints on SUSY, on the full superpotential, including B- and L-violating operators. The MFV hypothesis in effect imposes an accidental approximate R-parity on the first two generations and greatly suppresses dangerous operators such as those that induce proton decay. At the same time, there are non-trivial R-parity violating (RPV) couplings involving the third generation which are sufficient to render the LSP unstable on collider time scales and weaken the LHC bounds. This is the framework that we focus on in this section.*

As for any SUSY model, the collider phenomenology of MFV SUSY depends sensitively on the superpartner spectrum. This, in turn, is determined by the details of the SUSY breaking sector and mediation, for which many possible models have been proposed. In this section, we focus on a simple scenario motivated by bottom-up naturalness considerations. It is well known that the only superpartners required to be light ($\lesssim 1$ TeV) by naturalness are the stops $\tilde{t}_{1,2}$, the Higgsino $\tilde{H}$, and the gluino $\tilde{g}$: see, for example, [30] for a clear and careful explanation of this point. Of these, $\tilde{H}$ has a suppressed production rate due to its weak coupling. Thus, it will not have a considerable impact on phenomenology as long as it is not the LSP. We will therefore consider a simplified model [12] with just two states: a gluino $\tilde{g}$ and a stop $\tilde{t}$. All other SUSY particles are assumed to be either too heavy or too weakly coupled to be relevant at the LHC.† We assume that the stop is the LSP, as motivated by naturalness considerations, and that $m_{\tilde{g}} > m_{\tilde{t}} + m_t$. We

*For recent work on complete SUSY models realizing this framework, see Refs. [77, 63, 49].

†We do not include a left-handed sbottom $\tilde{b}_L$ in our simplified model even though its presence at the same mass scale as the stop is well motivated. In MFV SUSY, the dominant sbottom decays typically involve the top quark, $\tilde{b} \to tc$ or $\tilde{b} \to t\tilde{\chi}^-$, so that gluino cascades via sbottoms can still produce the same-sign dilepton signature. Thus we expect that the bounds derived here would qualitatively apply to most MFV SUSY models with $m_{\tilde{g}} > m_{\tilde{b}}$ as well.

focus on gluino pair-production, $pp \to \tilde{g}\tilde{g}$, followed by a cascade decay:

$$\begin{aligned} \tilde{g} &\to \tilde{t}\overline{t}, \quad \tilde{t} \to \overline{b}\overline{s}, \\ &\text{or} \\ \tilde{g} &\to \tilde{t}^* t, \quad \tilde{t}^* \to bs. \end{aligned} \tag{3.1}$$

The branching ratio for each of these channels is 50%, assuming a purely Majorana gluino. With probability of 50%, the gluino pair will produce a same-sign top pair (tt or $\overline{t}\overline{t}$). If each top decays leptonically, the final state will contain two same-sign leptons: $e^{\pm}e^{\pm}$, $\mu^{\pm}\mu^{\pm}$, or $e^{\pm}\mu^{\pm}$. Such "same-sign dilepton" (SSDL) events are very rare in the SM, and the SSDL signature already plays a prominent role in the LHC SUSY searches. Typically, these searches demand substantial MET in addition to SSDL, reducing their sensitivity to the RPV cascades (3.2) where the only sources of MET are neutrinos from leptonic top decays. However, the SSDL signature by itself is so striking that searches may be conducted even with no (or very low) MET cut, making them sensitive to RPV SUSY [10, 23, 14, 67].[‡] The first goal of this section is to estimate the current bounds on our simplified model using the latest publicly available CMS search for the SSDL signature [44]. This search uses 10.5 fb^{-1} of data collected at $\sqrt{s} = 8$ TeV in the 2012 LHC run.

While the current SSDL searches already place interesting bounds on RPV SUSY, they are not optimized for this class of models. The second goal of this section is to suggest ideas for optimizing this search that may be implemented by the experiments in the future. SSDL events in RPV SUSY have at least 6 parton-level jets. This high jet multiplicity can, by itself, provide an additional handle to suppress backgrounds. Moreover, two pairs of these jets come from stop decays. Depending on the gluino and stop masses, two regimes are possible. If $m_{\tilde{g}} - m_{\tilde{t}} \sim m_t$, the stops are typically non-relativistic in the lab

[‡]Other signatures of RPV SUSY with light stops and gluinos have been discussed in [52, 76, 31, 61, 64, 42, 3]. SSDL signature from resonant slepton production has been discussed in [56].

frame and the two jets are well separated. In this regime, one simply needs to look for a resonance in the dijet invariant mass. The case $m_{\tilde{g}} \gg m_{\tilde{t}}$ is more interesting. In this case, the stops are predominantly relativistic, and their decay products are boosted in the direction of their motion. The two parton showers would typically be merged in a single jet, and the signatures of their "stoppy" origin are hidden in the *substructure* of the jet. Recently, much work has been done on exploring observables sensitive to jet substructure (for a review, see [11]). We will show how some of these techniques can be used to further enhance the sensitivity of the SSDL search for RPV SUSY.

The rest of the section is organized as follows. The current bounds on RPV SUSY derived from the recently published CMS search in the SSDL channel are presented in Section 3.1.2. Additional cuts that can be used to improve the sensitivity of this search specifically in the RPV SUSY case are discussed in Section 3.1.3. Section 3.1.4 contains brief conclusions and outlook, while some of the details of the procedure used to recast the CMS search are presented in Appendix A.

3.1.2 Current Bounds: Recasting the CMS SSDL Search

Both CMS and ATLAS perform searches for the SSDL signature, accompanied by MET and jets (with or without b-tag requirement), as part of their standard search strategy to look for R-parity conserving (RPC) SUSY with light gluinos and stops. These analyses have non-trivial sensitivity to the RPV SUSY cascade (3.2) since leptonic top decays contain neutrinos which provide genuine MET, typically in the few tens of GeV range. While most RPC SUSY searches must impose a MET cut of at least 100 GeV to suppress SM backgrounds, the SSDL signature by itself is very rare in the SM so that such a strong MET cut is not required. The CMS collaboration recently published bounds based on a number

	SR0	SR1	SR2	SR3	SR4	SR5	SR6	SR7	SR8
No. of jets	≥ 2	≥ 2	≥ 2	≥ 4	≥ 4	≥ 4	≥ 4	≥ 3	≥ 4
No. of b-tags	≥ 2	≥ 2	≥ 2	≥ 2	≥ 2	≥ 2	≥ 2	≥ 3	≥ 2
ℓ charges	$++/--$	$++/--$	$++$	$++/--$	$++/--$	$++/--$	$++/--$	$++/--$	$++/--$
$\not{E}_T$	> 0 GeV	> 30 GeV	> 30 GeV	> 120 GeV	> 50 GeV	> 50 GeV	> 120 GeV	> 50 GeV	> 0 GeV
H_T	> 80 GeV	> 80 GeV	> 80 GeV	> 200 GeV	> 200 GeV	> 320 GeV	> 320 GeV	> 200 GeV	> 320 GeV

Table 3.1: Event characteristics required in the 9 signal regions (SRs) used in the CMS SSDL+MET+b analysis [44]. Note that the number of jets on the first line of the table includes both b-tagged and non-b-tagged jets. For the predicted background rates and the observed rates in each region, see Table 2 of [44].

of signal regions (SRs) with either no MET cut or sufficiently low MET cuts (30–50 GeV) that are easily exceeded by the top-induced MET [44]. While the CMS paper interprets the results in terms of RPC SUSY, it is straightforward to "recast" their published data to provide limits on the RPV case.[§]

The cuts imposed by the CMS analysis are summarized in Table 3.1. The acceptance cuts are $p_T > 40$ GeV, $|\eta| < 2.4$ for jets (both b-tagged and non-b-tagged), and $p_T > 20$ GeV, $|\eta| < 2.4$ for electrons and muons. Electrons are also not accepted at $1.442 < |\eta| < 1.566$ due to a gap in EM calorimeter coverage. Events with a third lepton are vetoed if they contain an opposite-sign lepton pair with invariant mass below 12 GeV, or between 76 and 106 GeV, to avoid contamination from Z decays. For more details on the CMS analysis, see [44].

In all nine signal regions, the data is consistent with the SM expectation, so an upper bound on the number of signal events can be set. We simulated the process $pp \to \tilde{g}\tilde{g}$, followed by the decays (3.2) and the leptonic top decay on both sides, using `Pythia 8.162` [92], for a large set of $(m_{\tilde{g}}, m_{\tilde{t}})$ points. The leading order (LO) cross section provided by `Pythia` is multiplied by the NLO K-factor computed with `Prospino 2.1` [22] for normalization. To compute the efficiency of the CMS cuts on the signal, we essen-

[§]Previous recasts of the LHC SSDL searches in terms of RPV SUSY have appeared in [10, 67]. These searches use smaller data sets than the one considered here.

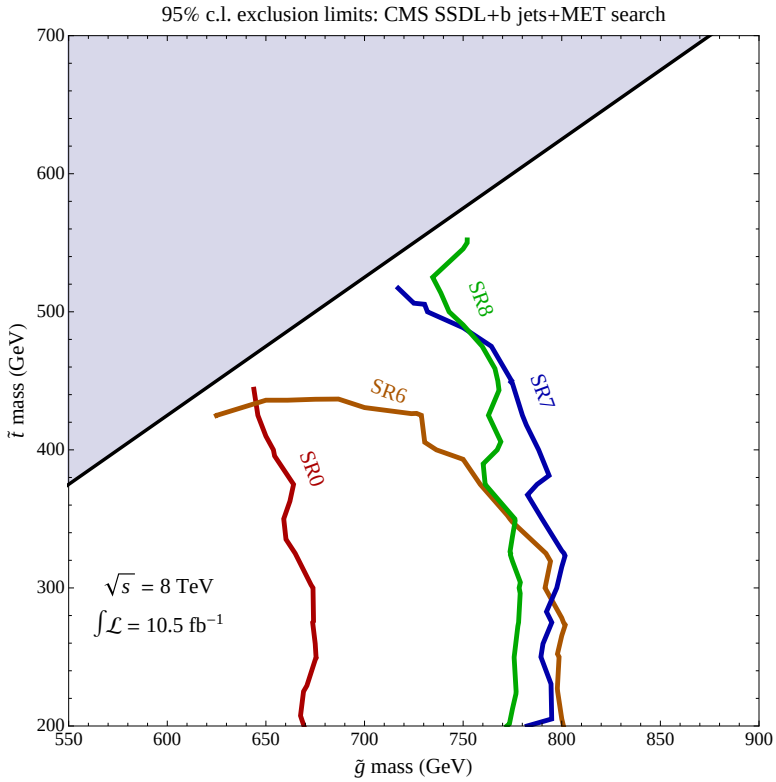

Figure 3.1: 95% CL exclusion of the RPV SUSY simplified model parameter space, based on the 4 most sensitive search regions (SRs) from the CMS SSDL+MET+b search [44] with 10.5 fb^{-1} of data collected at the 8 TeV LHC.

tially follow the procedure described in the CMS report [44] and its predecessors [41, 46]. For details, see Appendix A. The only non-trivial deviation from the CMS prescriptions concerns the treatment of lepton selection efficiencies. These have two factors: identification (ID) efficiency and the efficiency of the lepton isolation cut. CMS only published the combined lepton selection efficiency for a benchmark RPC SUSY point LM9 [21]. However, the RPV SUSY signal is expected to have a significantly different lepton isolation efficiency: there is more hadronic activity, and, in some parts of the parameter space, the tops are boosted, resulting in a b-jet in close proximity to the lepton. To take this into account, we estimate the lepton isolation cut efficiency from our signal MC, at each $(m_{\tilde{g}}, m_{\tilde{t}})$ point, and multiply by the lepton ID efficiency estimated by a separate simulation of the LM9 RPC SUSY signal. The cross section, acceptance and efficiency are then used to

compute the number of expected signal events at each $(m_{\tilde{g}}, m_{\tilde{t}})$ point. Comparing this number with the background prediction and data provided by CMS and using the CL_s method [71, 88] yields the expected 95% confidence level (CL) exclusion.

The results of this analysis are summarized by Fig. 3.1, which shows the 95% CL exclusion contours from the four most sensitive signal regions. We conclude that the current bound on the gluino mass is about 800 GeV. The bound is approximately independent of the stop mass as long as an on-shell decay $\tilde{g} \to \tilde{t}t$ is kinematically allowed. Note that this bound is somewhat stronger than the bound recently obtained in [67] by recasting the ATLAS SSDL+MET+j search [1]. The difference is especially pronounced in the region of relatively small gluino/stop mass splitting, where the ATLAS analysis loses sensitivity due to the large MET required (≥ 150 GeV). The remaining differences are accounted for by the slightly higher integrated luminosity of the CMS search, as well as the additional requirement of b-tagged jets imposed by CMS.

3.1.3 Future Searches: Optimizing for the RPV

While the current SSDL+MET+b searches already provide meaningful bounds on RPV SUSY, they are clearly not optimized for this model. In this section, we suggest ways to enhance their sensitivity to the RPV model, and demonstrate the improvements with a Monte Carlo analysis.

The key observation is that in a large section of the available parameter space, the stops produced in the gluino decays are relativistic. The stop boost in the gluino rest frame is given by

$$\gamma = \frac{1}{\sqrt{1-\beta^2}} = \frac{m_{\tilde{g}}^2 + m_{\tilde{t}}^2 - m_t^2}{2 m_{\tilde{g}} m_{\tilde{t}}} \tag{3.2}$$

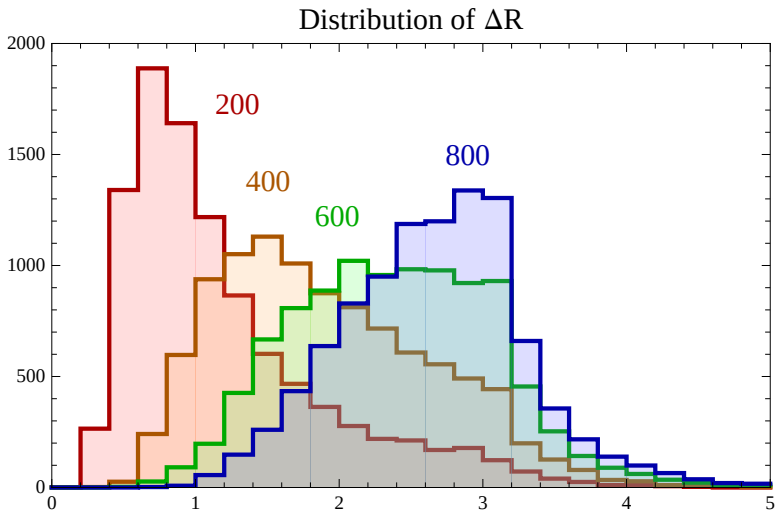

Figure 3.2: Lab-frame angular separation between the two quarks from a stop decay. The stops are produced in the gluino cascade (3.2), following gluino pair-production at a 14 TeV LHC. We assume $m_{\tilde{g}} = 1.2$ TeV, and vary the stop mass: $m_{\tilde{t}} = 200, 400, 600$ and 800 GeV distributions are shown in red, orange, green and blue, respectively. The distributions were calculated using `MadGraph 5` [13].

so that stops are relativistic when $m_{\tilde{g}} \gg m_{\tilde{t}}$. For example, $m_{\tilde{g}} = 1.2$ TeV and $m_{\tilde{t}} = 200$ GeV yields $\beta \approx 0.9$. Since gluinos themselves are mostly produced with non-relativistic speeds in the lab frame, such stops are typically also relativistic in the lab frame. In this regime, the two quarks produced in the stop decay are boosted in the same direction and have a small angular separation as can be seen in Fig. 3.2. The showers produced by the neighboring quarks tend to be merged into a single jet. Such "stoppy" jets can be distinguished from regular QCD jets, as we will discuss in detail below, giving an extra handle that can be used to suppress the background and improve the search reach.

To assess the potential improvement, we performed a Monte Carlo study for the 14 TeV LHC. For this study, we simulated the signal, $pp \to \tilde{g}\tilde{g}$, using `Pythia 8.162` [92], for a large set of $(m_{\tilde{g}}, m_{\tilde{t}})$ points. The leading order (LO) cross section provided by `Pythia` is multiplied by the NLO K-factor for normalization. Gluino, top and W decays are also treated in `Pythia`, as are QCD initial radiation, showering and hadronization. Jet recon-

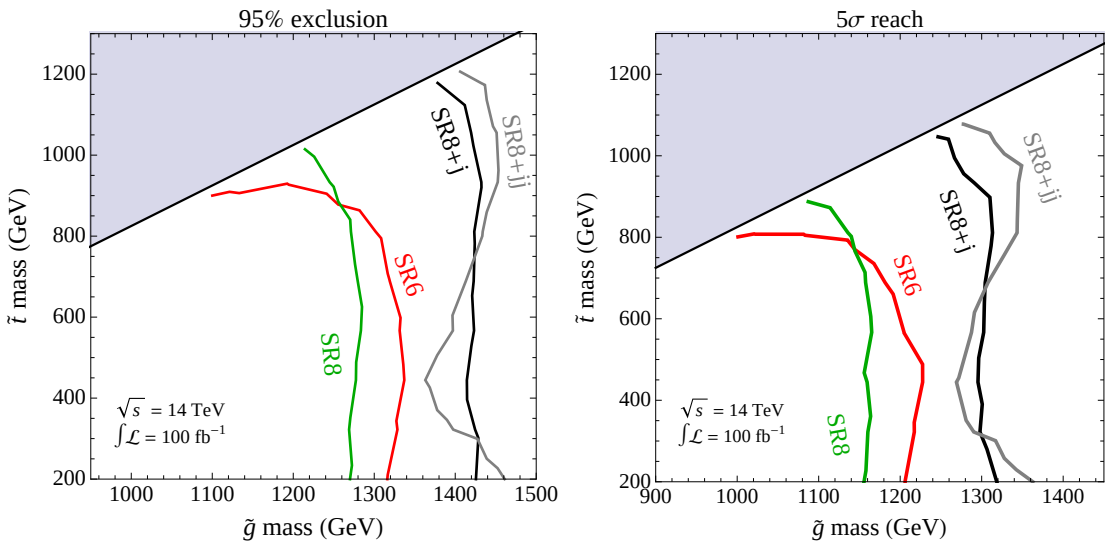

Figure 3.3: Estimated 95% CL expected exclusion (left panel) and 5σ expected discovery (right panel) reach in the RPV SUSY simplified model parameter space at the 14 TeV LHC with 100 fb^{-1}. Red/green lines: reach of the analysis identical to the one in [44], for signal regions SR6/SR8. Black/gray: reach of the analysis with the SR8 cuts and an additional requirement of one/two jets with $M_j > 175$ GeV. In the gray shaded region, the decay $\tilde{g} \to \tilde{t}t$ is kinematically forbidden.

struction is modeled with `FastJet` [36, 34] using the anti-k_T clustering algorithm. The dominant irreducible backgrounds, $t\bar{t}W$ and $t\bar{t}Z$, were simulated using the same tools. The cross sections for these processes are also normalized with NLO K-factors [37, 74].

To set a benchmark point against which improvements can be judged, we estimated the reach of the searches currently performed by CMS [44] at the 14 TeV LHC with $L_{\text{int}} = 100$ fb^{-1}. For this estimate, we implemented the cuts corresponding to the CMS signal regions listed in Table 3.1 (with the exception of SR7, which would require a separate analysis due to an additional b-tagged jet requirement) on both signal and background samples. We modeled b-tagging by applying a p_T-dependent tagging efficiency for the CSVM tagger [43] to all the jets that can be traced back to a b-hadron. The cut efficiencies for the signal and the background are listed in Table 3.2. We then estimated the instrumental background. The two dominant sources are "fake leptons" from sources

process	σ(total)	Eff(SR8)	σ(SR8)	Eff(1HMJ)	σ (SR8+1HMJ)	Eff(2HMJ)	σ (SR8+2HMJ)
signal $(1200, 200)$	113	0.41	0.46	86	0.40	40	0.18
$(1200, 500)$	114	0.44	0.50	64	0.32	24	0.12
$(1200, 800)$	114	0.45	0.52	70	0.36	31	0.16
$(1300, 200)$	63	0.36	0.23	89	0.20	40	0.09
$(1300, 500)$	63	0.48	0.30	71	0.22	22	0.07
$(1300, 800)$	63	0.45	0.28	75	0.21	31	0.09
$(1300, 1100)$	62	0.30	0.19	81	0.15	43	0.08
$(1400, 200)$	35	0.39	0.14	95	0.13	48	0.07
$(1400, 500)$	35	0.44	0.15	73	0.11	27	0.04
$(1400, 800)$	35	0.43	0.15	78	0.12	34	0.05
$(1400, 1000)$	35	0.45	0.16	81	0.13	43	0.07
$(1400, 1200)$	35	0.29	0.1	80	0.08	40	0.04
background $t\bar{t}W$	590	0.07	0.38	4.7	0.02	0.3	0.001
$t\bar{t}Z$	910	0.03	0.30	7.9	0.02	0.6	0.002

Table 3.2: Cross sections (in fb) and efficiencies (in %) of signal and background processes, at the 14 TeV LHC. The signal points are labeled by $(m_{\tilde{g}}, m_{\tilde{t}})$, both in GeV. The selection cuts are labeled as follows: SR8 refers to the cuts imposed by the CMS analysis [44] in signal region 8 (see Table 3.1); 1HMJ means requiring at least one "high-mass" jet ($M_j > 175$ GeV); similarly, 2HMJ requires at least 2 jets with $M_j > 175$ GeV. The 1HMJ and 2HMJ cuts are applied to the events that pass all SR8 cuts.

such as heavy-flavor decays and misidentified hadrons, and "charge flips", events with opposite-sign leptons where one of the charges is mismeasured. The ratio of the instrumental background to the irreducible component reported in [44] is roughly between 1:1 and 2:1, depending on the signal region. This indicates that instrumental backgrounds will play an important role at 14 TeV as well. Unfortunately, detailed modeling of these backgrounds requires either detector simulation or data-based techniques. However, a rough estimate may be obtained as follows. Since the physical process primarily responsible for the instrumental backgrounds is top pair-production[¶], it is reasonable to expect that the rates scale approximately with the total $t\bar{t}$ cross section when the collision energy is increased from 8 to 14 TeV. Using this scaling and the instrumental background rates in various signal regions quoted in [44], we obtained corresponding estimates at 14 TeV. We found that the irreducible and instrumental background components scale by similar factors when going to 14 TeV: for example, our estimate of the instrumental/irreducible

[¶]We are grateful to Frank Wuerthwein for clarifying this point.

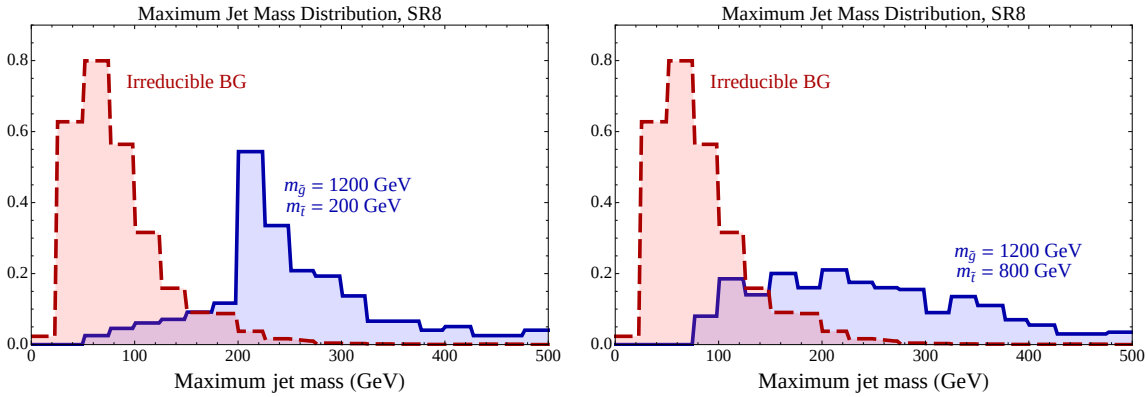

Figure 3.4: Distributions of the largest jet invariant mass $M_j^{\max}$, in the signal (blue) and irreducible background (red) events passing SR8 cuts at the 14 TeV LHC. The signal is simulated for $(m_{\tilde{g}}, m_{\tilde{t}}) = (1200, 200)$ GeV (left panel) and $(1200, 800)$ GeV (right panel). The background includes the SM $t\bar{t}W$ and $t\bar{t}Z$ processes.

ratio at 14 TeV for the signal region SR6 is 0.86, while for SR8 it is 1.62, quite close to the ratios at 8 TeV.

Combining the irreducible and instrumental backgrounds, we computed the exclusion levels expected under the assumption that the data exactly matches the background prediction, as well as the discovery reach defined by requiring at least a 5σ difference between the signal+background and background-only predictions. The estimated exclusion and discovery reach contours are shown in Fig. 3.3 for the two most sensitive signal regions: SR6 (red contour) and SR8 (green contour).

To identify the merged jets from stop decays, we first reclustered the samples, setting the jet opening angle to $\Delta R = 1.0$, as opposed to $\Delta R = 0.5$ used by the CMS analysis. Such "fat" jets are already being used by experimental analyses involving jet substructure (see, for example, [40, 2]). We then computed the invariant mass M_j of each jet. The distributions of the largest M_j in each event, for both the signal and the (irreducible) background samples, are shown in Fig. 3.4. It is obvious that $M_j^{\max}$ is an excellent signal/background discriminator. For the case $m_{\tilde{g}} \gg m_{\tilde{t}}$, illustrated in the left panel of the

figure, the reason is obvious: the high-mass jets in the signal are due to boosted stop decays, and their masses peak around $m_{\tilde{t}}$. However, somewhat more surprisingly, this discriminator continues to work well in the regime $m_{\tilde{g}} \sim m_{\tilde{t}}$, as illustrated by the right panel of the figure. The reason for this is simply the large jet multiplicity in the signal, which at parton level has 6 quarks in the final state. In this situation, two independent parton showers (from different stops, or from a stop and a top) often get accidentally merged into a single jet which is more likely to have a large invariant mass than a single-parton QCD jet. (This phenomenon was previously noticed in [69, 45].) As a result, requiring massive jet(s) improves the reach of the search throughout the parameter space, and not just for large $m_{\tilde{g}}/m_{\tilde{t}}$.

The improvement of the reach with the jet mass cut is shown by the black and gray lines in Fig. 3.3. This analysis imposes all of the SR8 cuts with the additional requirement of at least one or two high-mass jets with $M_j > 175$ GeV. The efficiencies of these cuts, and cross sections after all cuts, are listed in Table 3.2. For the reach estimate, we assumed that the efficiency of the jet invariant mass cuts on the instrumental and irreducible backgrounds are the same (which seems reasonable since both contain QCD jets of similar energies). We found that gluinos up to $1.4 - 1.45$ TeV can be excluded at the 95% CL, while gluinos up to $1.3 - 1.35$ TeV can be discovered at the 5σ level at the 14 TeV LHC with 100 fb^{-1}. The dependence of the reach on the stop mass is quite weak, especially when the analyses with ≥ 1 and ≥ 2 high-mass jets are combined.

An even stronger separation of signal and background can be achieved by noticing that the high-mass jets in the background are primarily due to boosted, fully hadronic tops. Such jets have three hard partons. In contrast, the signal jets typically have two hard partons from a two-body stop decay. To exploit this, we used the N-subjettiness technique proposed by Thaler and Van Tilburg [95]. In this approach, observables τ_N are defined

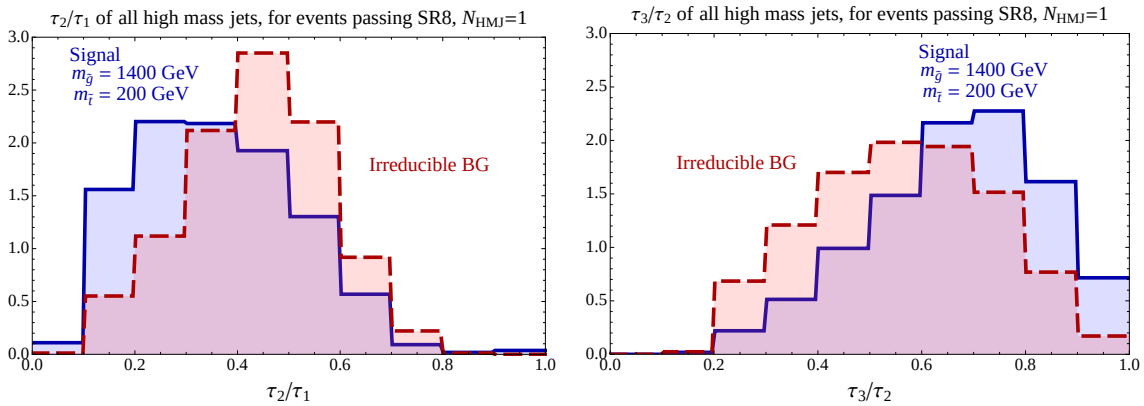

Figure 3.5: Distributions of N-subjettiness observables, τ_2/τ_1 (left) and τ_3/τ_2 (right), for the high-mass jets ($M_j > 175$ GeV) in the signal (blue) and irreducible background (red) events passing SR8 cuts. The signal is simulated for $(m_{\tilde{g}}, m_{\tilde{t}}) = (1400, 200)$ GeV. All distributions are normalized to unit area.

with $N = 1, 2, \ldots$. A low value of the ratio τ_N/τ_{N-1} indicates that the jet likely has an N-pronged substructure. For example, the distributions of jets with $M_j > 175$ GeV in τ_2/τ_1 and τ_3/τ_2 observables are shown in Fig. 3.5, where in the signal simulation we assumed $(m_{\tilde{g}}, m_{\tilde{t}}) = (1400, 200)$ GeV, and used the `onepass_kt_axes` minimization scheme and $\beta = 1.1$. As expected, low values of τ_2/τ_1 are favored in the signal, while low values of τ_3/τ_2 are favored in the background. It should be noted that with the 100 fb^{-1} data set, the reach of the jet-mass based searches shown in Fig. 3.3 is already statistics-limited, so no further improvement can be achieved by cutting on the N-subjettiness observables. However, they can be useful for larger data sets, or as a part of more globally optimized set of cuts.

Since no detector simulation could be performed for this study, our instrumental background estimate is clearly very crude and has a large uncertainty. To illustrate how this uncertainty affects the reach of the proposed search, we define

$$\zeta = \frac{\text{Total BG Rate}}{\text{Irreducible BG Rate}}, \tag{3.3}$$

where both rates include all the cuts imposed in a particular analysis. Fig. 3.6 shows the

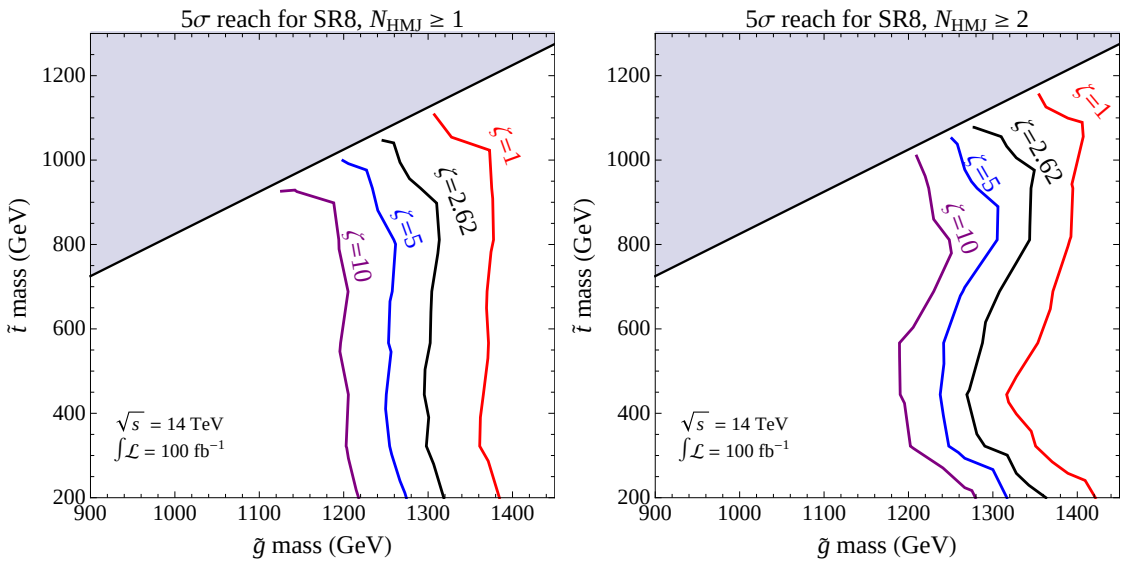

Figure 3.6: Estimated discovery reach in the RPV SUSY simplified model parameter space, at the 14 TeV LHC with 100 fb^{-1} of data, for a range of assumptions concerning the instrumental background. The selection cuts are SR8, plus ≥ 1 (left) or ≥ 2 (right) jets with $M_j > 175$ GeV. The value $\zeta = 2.62$ is the estimate obtained by rescaling from 8 TeV and used in Fig. 3.3. In the gray shaded region, the decay $\tilde{g} \to \tilde{t}t$ is kinematically forbidden.

variation of the reach for values of ζ between 1 and 10, for the same analysis as in Fig. 3.3 (SR8 plus ≥ 1 or ≥ 2 jets with $M_j > 175$ GeV). The reach estimates are relatively robust with respect to the uncertainty in the instrumental background estimate, due to a strong dependence of the signal rates on $m_{\tilde{g}}$.

3.1.4 Discussion and Conclusions

The main results of this section can be summarized as follows:

- The current CMS searches for anomalous events with SSDL and b-jets place a lower bound of about 800 GeV on the gluino mass in the gluino-stop simplified model of RPV/MFV SUSY. The bound is only weakly sensitive to the stop mass, as long as an

on-shell decay $\tilde{g} \to \tilde{t}t$ is kinematically allowed.

- A search identical to the current CMS search, implemented at the 14 TeV LHC with 100 fb^{-1} of data, is estimated to have the sensitivity to exclude gluino masses up to about 1.3 TeV at the 95% CL, and a 5σ discovery reach of about 1.2 TeV. Again, these are largely insensitive to the stop mass.
- An addition of a cut on the jet invariant mass improves the 95% CL exclusion reach and the 5σ discovery reach to approximately 1.45 TeV and 1.35 TeV, respectively. While the improvement in terms of the gluino mass is only about 10% in both cases, it is still very significant since the gluino cross section drops very rapidly with mass.

While the motivation for our analysis comes primarily from the MFV SUSY model [48], the results apply quite generally to RPV models with a stop LSP, decaying via a UDD-type operator. (See, for example, [27] for a recent discussion of such models.) A non-MFV flavor structure of the stop decay operator may result in fewer b-jets, but since top quarks still provide two genuine b-jets per event, even in this case the efficiencies of the cuts should not be strongly degraded.

For our signature to work, it is crucial that the gluino be a Majorana particle. If the gluino is Dirac, no SSDL signature is possible, and other handles must be used to suppress the SM background. However, high-mass jets from stop decays are still present in this situation, and can provide a useful discriminant [67]. It would be interesting to see if, in addition to stop jets, massive jets formed by the boosted SM tops produced from the same gluino decays can be useful in this context. (The utility of boosted top-jets in searching for the gluino-stop cascade decays in R-parity conserving SUSY has been pointed out in [24].) We leave this possibility for future study.

3.2 Snowmass 2013: RPV SUSY with Same-Sign Dileptons at LHC-14

3.2.1 Introduction

Experiments at the 8 TeV run of the Large Hadron Collider (LHC-8) did not discover evidence for supersymmetry (SUSY), placing stringent lower bounds on the masses of many of the superpartners. In a completely natural theory, some of the superpartners are required to be in the few hundred GeV to a TeV range independently of the details of SUSY breaking. In particular, such model-independent upper mass bounds apply to stops $\tilde{t}$ and gluinos $\tilde{g}$ (see, for example, [30]). In the "standard" realization of SUSY, with conserved R-parity and a weakly interacting lightest supersymmetric particle (LSP), the LHC experiments already strongly constrain this possibility. This motivates interest in alternative realizations of SUSY, including models with R-parity violation (RPV), which will be our focus in this section. On the theoretical side, an attractive scenario, "MFV SUSY", has been proposed [48, 80]. In this model, RPV is confined almost exclusively to third-generation quarks, avoiding the bounds from the non-observation of baryon number violating processes. On the experimental side, RPV SUSY predicts events with no large missing transverse energy (MET), making it much more difficult to distinguish SUSY events from Standard Model (SM) backgrounds and thus avoiding most LHC constraints.

Even though the standard large-MET cuts are not useful in RPV SUSY searches, other handles can be used. In this section, we will focus on the same-sign dilepton signature, proposed in [10, 25, 59]. (For other signatures, see for example [61, 67, 57, 16].) Consider a simplified RPV model with a stop LSP and a gluino in the TeV mass range, as motivated by naturalness. In simple SUSY models, the gluino is a Majorana particle, so that both

decays

$$\tilde{g} \to \tilde{t}\bar{t}, \quad \tilde{g} \to \tilde{t}^* t \tag{3.4}$$

are possible and occur with the same probability. Gluino pair-production at the LHC can then lead to events with two *same-sign* tops, and if each of them decays leptonically, the same-sign dilepton (SSDL) signature is obtained. The stops decay via an RPV operator $\tilde{t} \to \bar{b}\bar{s}$, as predicted by the MFV SUSY scenario, so that no large MET is produced. (A small amount of MET is always present from neutrinos in leptonic top decays.) Nevertheless, this signature has a very small SM background, and provides a promising search channel. The 95% c.l. bound on the gluino mass, estimated in [25] based on a CMS search [44] using 10.5 fb^{-1} of LHC-8 data, is about 800 GeV, approximately independent of the stop mass as long as the decay (3.4) can occur on-shell. Recently, this search strategy was implemented by the CMS collaboration in [47], yielding the gluino mass bound of 900 GeV with the full 2012 data set. The CMS analysis assumed that the decay (3.4) is off-shell.

3.2.2 Analysis Setup

We estimate the sensitivity of the SSDL search for RPV SUSY at the next run of the LHC, for which we assume the center-of-mass energy of 14 TeV. To perform this estimate, we simulate signal events, for a set of 198 parameter points in the $(m_{\tilde{g}}, m_{\tilde{t}})$ plane, using `PYTHIA 8` [92]. Signal cross sections are scaled up to NLO using K-factors calculated in `Prospino 2.1` [22]. For gluino masses higher than what Prospino can calculate, we estimate the K-factors by linear extrapolation. We approximately model the detector response with `Delphes 3` [51], and apply an analysis based on the work in [25]. Pile-up effects are not included in this analysis.

The Delphes detector simulation is controlled by a modified version of the default CMS card included in Delphes. Particle propagation, tracking efficiencies, energy and momentum smearing, and calorimeter response are left unchanged. We require leptons to have $p_T > 20$ GeV and $|\eta| < 2.4$ (excluding electrons in the ECAL gap, $1.442 < |\eta| < 1.566$). We then apply an identification efficiency (73% for e, 84% for μ) calculated in Appendix A of [25] from the data in [44], and an isolation cut requiring the scalar p_T sum of all objects within $\Delta R = \sqrt{(\Delta\eta)^2 + (\Delta\phi)^2} = 0.3$ of the lepton to be no greater than 10% of the lepton's p_T. We cluster fat jets with the anti-kt algorithm implemented in `FastJet 3` [36, 34], with $R = 1.0$, and require them to have $p_T > 40$ GeV and $|\eta| < 2.4$. For b-tagging, we use the tagging and mistagging efficiencies for the CSVM tagger from [43]. Finally, we also tag jets with masses above the top mass as "high-mass jets".

After the detector simulation, we select the same-sign lepton pair with the highest p_T and pair invariant mass greater than 8 GeV to be our "SSDL pair". We apply a dilepton trigger efficiency of 96% for ee, 93% for $e\mu$, and 88% for $\mu\mu$ [44]. We veto events where a third lepton, with $p_T > 10$ GeV and isolation sum no greater than 20% of the lepton's p_T, forms an opposite-sign same-flavor pair with one of the SSDL pair leptons, with a pair invariant mass between 76 and 106 GeV, to remove background events with leptons from Z decays. We also veto events where a third lepton, with $p_T > 5$ GeV and isolation sum no greater than 20% of the lepton's p_T, forms an opposite-sign same-flavor pair with one of the SSDL pair leptons, with a pair invariant mass below 12 GeV, to remove background events with leptons from a γ^* or a low-mass bound state.

For an event to pass the analysis cuts, we require that an SSDL pair is found, and then we apply the event-level cuts for each of the signal regions used in the current CMS search, see Table 2 of [44], except for SR7. Additionally, we require either $N_{HMJ} \geq 1$ or $N_{HMJ} \geq 2$, where N_{HMJ} is the number of high-mass jets in the event. To estimate the

sensitivity of this search at LHC-14, we compare the projected reach for all 8 signal regions we implemented, with two N_{HMJ} choices for each one. We select the most sensitive among these choices. However, we did not attempt to optimize the cuts further by going beyond the settings of the current CMS search; such optimization can of course only improve the reach.

Irreducible backgrounds to this search involve processes that can generate two prompt same-sign leptons. To model them, we generate 500K events each of $t\bar{t}W^{\pm}$ and $t\bar{t}Z$ in `MadGraph 5` [13], and scale their cross sections up to NLO with K-factors 1.236 [37] and 1.387 [74], respectively. These events are put through the same hadronization, detector simulation, and analysis as the signal events.

Instrumental backgrounds to this search mainly involve "fake leptons" from heavy-flavor decays and misidentified hadrons, and "charge flips" where an opposite-sign dilepton event has one of its lepton charges mismeasured. These dominantly arise from top pair-production. Since both effects are rare, a very large sample of $t\bar{t}$ Monte Carlo events would be required to estimate their rates from simulation. In this preliminary study, we instead estimate the instrumental background by noting the rates in each of the signal regions in Table 2 of [44] and assuming that they scale with the $t\bar{t}$ cross section when the collision energy is increased from 8 to 14 TeV. Previous study in [25] showed that the resulting reach is not heavily sensitive to this assumption. We combine the irreducible and instrumental backgrounds to arrive at the total background for each signal region and choice of N_{HMJ} cut.

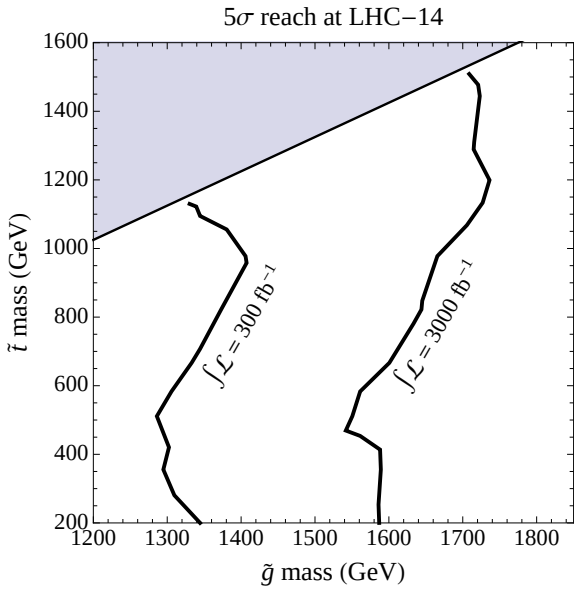

Figure 3.7: Estimated 5σ reach of LHC-14 in the RPV SUSY simplified model.

3.2.3 LHC Sensitivity at $\sqrt{s} = 14$ TeV

The projected sensitivity of the LHC-14 in the $(m_{\tilde{g}}, m_{\tilde{t}})$ plane is shown in Figure 3.7. We find that among the CMS signal regions, SR5, with the additional requirement of 2 high-mass jets, gives the best sensitivity, although several other SRs are almost as sensitive. Significant improvements of the reach compared to the present exclusion bounds can be clearly achieved: for example, with 300 fb^{-1} of data, the 5σ reach in gluino mass is as high as 1.4 TeV, approximately independent of $m_{\tilde{t}}$. If the High Luminosity (HL) LHC upgrade is implemented and yields 3 ab^{-1} of data, the reach can be further increased to $1.6 - 1.75$ TeV depending on $m_{\tilde{t}}$. Note that for technical reasons, our analysis has been restricted to the part of parameter space where the decays (3.4) occur on-shell. However, the analysis should retain sensitivity even in the region where the gluinos decay in a single-step, three-body channel $\tilde{g} \to tbs$.

In summary, same-sign dilepton (SSDL) signature provides a promising channel to

search for RPV supersymmetry, within the gluino/stop simplified model motivated by naturalness. We find that experiments at the LHC-14 can achieve impressive sensitivity for this model, especially if a large data set becomes available with the HL upgrade.

CHAPTER 4

LOOKING BEYOND THE PHENOMENOLOGY

The SUSY-Yukawa sum rule [28] had previously been proposed as a probe of the mechanism that cancels quadratic divergences that threaten to destabilize the Higgs mass. This cancellation uniquely fixes a particular combination of stop and sbottom masses and mixing angles, which they denoted Υ, at tree-level. However, radiative corrections make the prediction for Υ dependent on other SUSY parameters. It thus became important to determine how much Υ is allowed to vary over the allowed parameter space. While a brute-force scan over this multidimensional space is beyond our computational capabilities, Markov chain Monte Carlo (MCMC) allows us to efficiently sample regions of the space that are consistent with experimental measurements, and extract the Υ distribution.

This chapter is based on the talk *SUSY-Yukawa Sum Rule at the LHC and the ILC* [82], based on work in collaboration with Maxim Perelstein, given at the 2011 International Workshop on Future Linear Colliders (LCWS11) in Granada, Spain.

4.1 SUSY-Yukawa Sum Rule at the LHC and the ILC

4.1.1 Introduction

Supersymmetry (SUSY) is the only known mechanism which removes the quadratic divergence in the Higgs mass to all orders in perturbation theory, allowing the theory to remain perturbative to very high energy scales, such as GUT or Planck scale, without fine-tuning. SUSY predicts a number of new particles, with masses generically at the TeV scale, and searches for such particles are a major part of the LHC physics program. If such superparticles are within reach of the ILC, their masses and some of the couplings can be measured with high precision [7]. The couplings between superpartners and the Higgs would be particularly important to measure, since they are unambiguously fixed by the requirement of quadratic divergence cancellation, and measuring them gives a unique test of the SUSY solution to the hierarchy problem. By the same token, these couplings are extremely model-independent: as long as the underlying mechanism of hierarchy stabilization is SUSY, they cannot be changed, while most other observables (superparticle spectrum, decay channels, etc.) depend on details of the SUSY model and breaking mechanism. The strongest of such couplings is the Higgs coupling to the superpartners of the top, the stop bosons, since it is related to the top Yukawa, the strongest coupling of the Standard Model Higgs. Can this coupling be measured, at the LHC or the ILC?

On the one hand, there are reasons to be optimistic: naturalness suggests that stops must be rather light, ideally in the 300–400 GeV range, if SUSY is indeed responsible for stabilizing the Higgs [30]. (Note also that, at the time of this writing, this mass range is not excluded by the LHC searches, as long as stops are significantly lighter than all other squarks [30, 81].) On the other hand, a direct measurement of the $hh\tilde{t}\tilde{t}$ vertex appears

impossible, since the processes containing this vertex and quarks, gluons or electrons in the initial state have very small cross sections. The solution to this was proposed in [28], where a simple sum rule was formulated. The sum rule is a direct consequence of the SUSY relation between the top Yukawa and the $hh\tilde{t}\tilde{t}$ vertex, and at the same time it is made up entirely of potentially observable quantities, such as masses and mixing angles of the third-generation squarks. In this section, we will briefly describe the sum rule, and outline the prospects for testing it at the LHC [28]. We will also describe how the LHC and ILC measurements of SUSY parameters outside of the third-generation squark sector can sharpen the theoretical prediction of the sum rule, by providing crucial information about the size of the radiative corrections to the sum rule. Finally, we will argue that an e^+e^- collider, such as the ILC (or a higher-energy machine, if necessary to pair-produce stops and sbottoms) would be required to get sufficient information about the third-generation squark sector to unambiguously test the sum rule.

4.1.2 SUSY-Yukawa Sum Rule

The couplings of the Higgs to top and its partners, stops $\tilde{t}_L$ and $\tilde{t}_R$, have the form

$$\mathcal{L} \supset \frac{y_t}{\sqrt{2}} h\bar{t}t + \frac{y_t^2}{2} h^2(|\tilde{t}_L|^2 + |\tilde{t}_R|^2), \tag{4.1}$$

where y_t is the top Yukawa constant. It is crucial for divergence cancellation, and guaranteed by SUSY, that the same y_t appears in the two terms; the task is to test this fact experimentally. To our knowledge, a direct experimental measurement of the strength of the quartic interaction $hh\tilde{t}\tilde{t}$ is impossible. Once the Higgs gets a vev, $\langle h \rangle = v$, a cubic interaction $h\tilde{t}\tilde{t}$ is generated, but it also seems very difficult to measure (although in some special cases this may be possible [38]). A mass term, $y_t^2 v^2(|\tilde{t}_L|^2 + |\tilde{t}_R|^2)$, is also generated, giving a mass precisely equal to m_t to both stops. If this was the only con-

tribution to the stop masses, it could be easily measured, providing a somewhat indirect but still very robust confirmation of the structure of Eq. (4.1). Of course, there are other contributions: the soft masses, $M_L^2|\tilde{t}_L|^2 + M_R^2|\tilde{t}_R|^2$, as well as the off-diagonal mass terms, $v(A_t \sin\beta - \mu\cos\beta)(\tilde{t}_L^* \tilde{t}_R + \text{c.c.})$, and the D-term contribution. Nevertheless, it was shown in [28] that the interesting contribution to the stop mass can be isolated and expressed in terms of physical observables. The SUSY prediction takes the form

$$\hat{m}_t^2 - \hat{m}_b^2 = m_{\tilde{t}1}^2 \cos^2\theta_{\tilde{t}} + m_{\tilde{t}2}^2 \sin^2\theta_{\tilde{t}} - m_{\tilde{b}1}^2 \cos^2\theta_{\tilde{b}} - m_{\tilde{b}2}^2 \sin^2\theta_{\tilde{b}} - m_W^2 \cos 2\beta, \tag{4.2}$$

where $\{\hat{m}_t, \hat{m}_b\}$ are the bare top and bottom masses, $\{m_{\tilde{t}a}, m_{\tilde{b}a}\}$ are the physical stop and sbottom masses ($a = 1, 2$), and $\{\theta_{\tilde{t}}, \theta_{\tilde{b}}\}$ are the rotation angles between the gauge and mass bases in the stop and sbottom sectors. This prediction was called "SUSY-Yukawa sum rule" in [28]. It is convenient to define a dimensionless quantity

$$\Upsilon \equiv \frac{m_{\tilde{t}1}^2 \cos^2\theta_{\tilde{t}} + m_{\tilde{t}2}^2 \sin^2\theta_{\tilde{t}} - m_{\tilde{b}1}^2 \cos^2\theta_{\tilde{b}} - m_{\tilde{b}2}^2 \sin^2\theta_{\tilde{b}}}{v^2} \tag{4.3}$$

to encapsulate the stop and sbottom sector masses and mixing angles, which have not yet been measured. SUSY predicts (at the tree level, in the large $\tan\beta$ limit)

$$\Upsilon_{\rm SUSY}^{\rm tree} = 0.28. \tag{4.4}$$

By measuring stop and sbottom sector masses and mixing angles, a task that's difficult but may not be impossible as we discuss below, this prediction can be tested.

Before proceeding, let us discuss loop corrections to the prediction (4.4). The masses in the definition of Υ are physical (pole) masses; one can also define the "running" version of this observable, $\Upsilon(\mu)$, which has the same form but with masses and mixings taking their running values evaluated at scale μ. The operations leading to the sum rule rely only on SUSY and $SU(2)_L$ gauge symmetry, so the tree-level sum rule applies to $\Upsilon(\mu)$ as long as μ is above SUSY and electroweak symmetry breaking scales. Thus, the only corrections

to the sum rule are threshold effects, with no large logs. Numerically, however, these corrections can be large, since the sum rule involves a delicate cancellation among the stop and sbottom terms, and even fractionally small corrections to each term can result in significant fractional corrections in Υ. This fact was already noted in [28], and will be further illustrated by the numerical work in the next section. This appears to diminish the usefulness of the sum rule. However, the large radiative correction is troublesome only if it is unknown; if it can be calculated and subtracted, the sum rule can still be meaningfully tested. Calculating the radiative corrections to the stop and sbottom masses requires knowledge of SUSY parameters, such as, for example, the gluino and chargino masses. In the next section, we show that experimental measurements of these masses at the LHC and ILC can significantly reduce the uncertainty on the theoretical prediction of Υ.

4.1.3 Improving the Theoretical Prediction of the Sum Rule with Data

While at tree level the SUSY prediction for Υ is just a fixed number (with only a slight $\tan\beta$ dependence), radiative corrections to Υ depend on a number of SUSY parameters. If these parameters are treated as unknown, SUSY prediction for Υ is significantly washed out, and a broad range of values is possible (see Fig. 2 in [28]). However, experimental measurement of SUSY parameters should clearly shrink this range. Testing the sum rule can then be thought of as consisting of two steps:

1. measure as many parameters as possible *not including third-generation squark masses and mixings*, and use them to narrow the range of possible radiative corrections to Υ, and

2. measure the third-generation squark masses and mixings, and check that the combination in Eq. (4.3) falls within the range determined in step 1.

In this section, we present a Monte Carlo study of step 1 of this procedure.

Our study is in the context of the phenomenological MSSM (pMSSM) [54]. We assumed that the "correct" model is the well-known benchmark point LCC1. We then scanned the pMSSM parameter space, and recorded the values of Υ at each point. To make efficient use of computing time, we only scan the parameters that significantly affect Υ, namely: M_1, M_2, M_3, $m_{\tilde{Q}}$, $m_{\tilde{t}_R}$, $m_{\tilde{b}_R}$, A_t, A_b, M_A (pole), $\tan\beta$ (m_Z), and μ. We fix all other parameters at their LCC1 values. Details on the parameter space are included in Appendix B.

Even with this simplification, the traditional method of scanning over a grid is computationally prohibitive, leading us to use Markov Chain Monte Carlo (MCMC) techniques as detailed in [17]. The MCMC algorithm is implemented in C++ with the GNU Scientific Library, and interfaces with SuSpect [55] for all the MSSM spectrum calculations. As in [17], we initialize 50 Markov chains around the benchmark point LCC1, propagate them for one million steps, burn the first 10% of each chain, and test for convergence of the algorithm with the Fourier analysis detailed in [58]. Details on the MCMC algorithm and its implementation are included in Appendix C.

We conducted three separate scans of the parameter space. The first scan does not assume any experimental knowledge of the superpartner masses, beyond the requirement of a neutralino LSP, the LEP constraints on charged superpartner masses (> 100 GeV) and the lightest CP-even Higgs mass (we use $m_h > 108$ GeV, to conservatively take into account the uncertainty of the SuSpect prediction), as well as the current experimental constraints on m_W, $g_\mu - 2$, and Br($b \to s\gamma$). (We do not take into account the dark matter

relic density constraint, which is subject to model-dependent cosmological uncertainties.) The top panel of Fig. 4.1 shows the resulting distribution of Υ.

We then repeated the scan with additional constraints on the SUSY parameters from measurements at the LHC-14 (middle panel) and the ILC-500 (bottom panel). We estimated the values of these measurements by using SuSpect to calculate the superpartner spectrum at the benchmark point LCC1. The estimates of the uncertainties in the LHC and ILC measurements are taken from the 2004 report of the LHC/LC study group [97] (for a concise summary of these estimates, see Table 2 of [17]). In all cases, we ignore information about third generation squarks, as explained above. Details on the constraints are included in Appendix B.

Figure 4.1 clearly demonstrates that, as expected, the "theoretical" prediction of Υ becomes sharper as more information on SUSY spectrum is gathered, allowing us to nail down the radiative corrections to stop and sbottom masses. It is useful to quantify this by computing the mean and standard deviation of the Υ predictions. Without any new experimental constraints from the LHC or ILC, $\Upsilon = 0.18 \pm 0.85$. After the LHC-14 measurements, it narrows to $\Upsilon = 0.37 \pm 0.39$, while the ILC measurements at $\sqrt{s} = 500\,\text{GeV}$ narrow it further to $\Upsilon = 0.42 \pm 0.19$. (The true value at LCC1 is $\Upsilon = 0.27$.)

Note that, at the time of this writing, the point LCC1 is already ruled out by the LHC data. It is clear that qualitative lessons of this study apply throughout the model parameter space, although of course the amount of information a given collider can obtain does depend strongly on the spectrum.

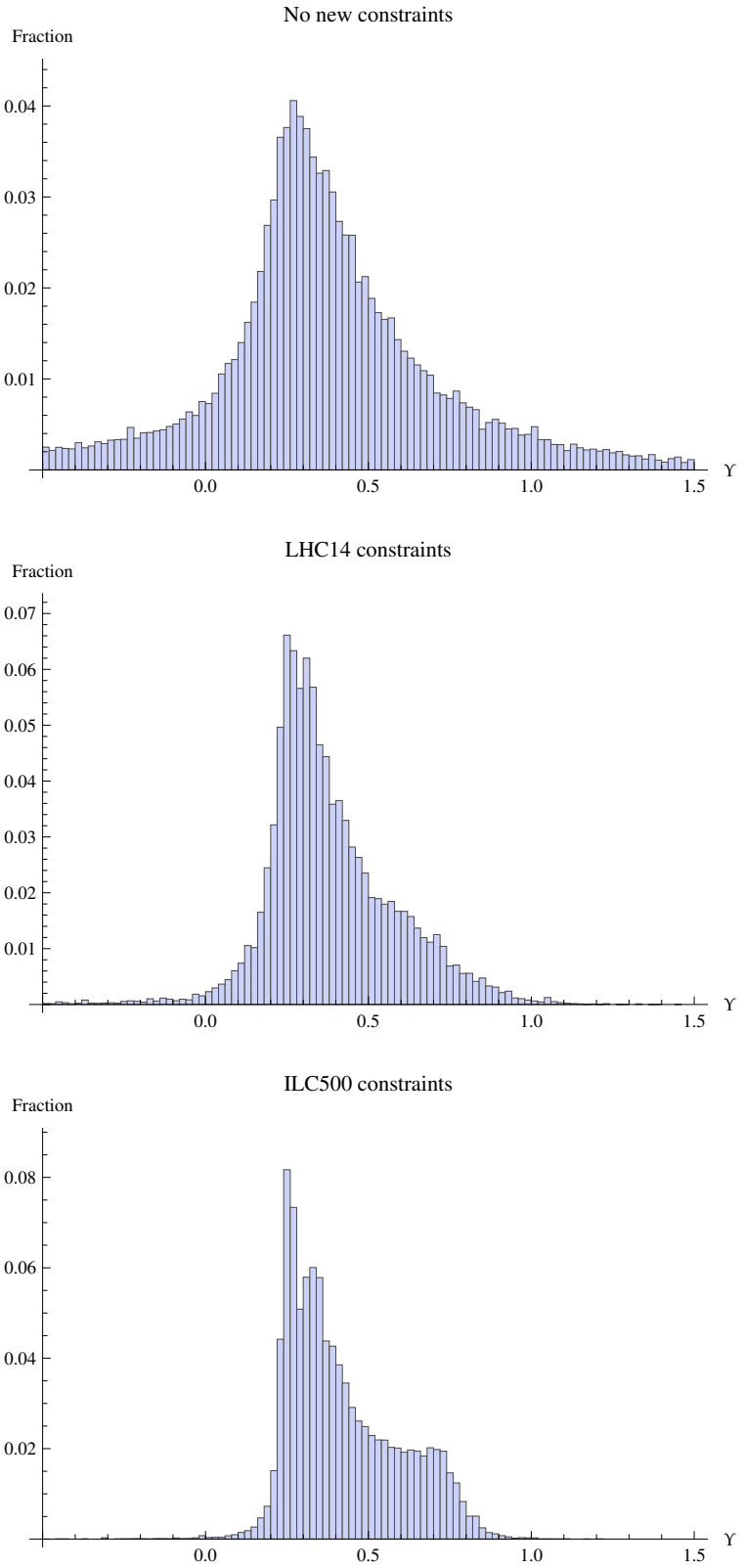

Figure 4.1: Distributions of Υ with different sets of experimental constraints. The assumed true model is the MSSM at the benchmark point LCC1.

4.1.4 Mass and Mixing Angle Measurements

To test the sum rule, the theoretical prediction discussed above must be compared to Υ computed by directly measuring stop and sbottom masses and mixing angles. [28] studied the potential for mass measurements at the LHC. The analysis relied on direct stop decays, $\tilde{t} \to t\tilde{\chi}_1^0$, and cascade decays of gluinos via sbottoms, $\tilde{g} \to \tilde{b}b$, $\tilde{b} \to b\tilde{\chi}_1^0$. Using the kinematic edge, as well as recently developed techniques such as subsystem M_{T2} variables [32], it was possible to extract the lighter stop and sbottom masses to roughly 10% accuracy at the benchmark point used in this study. Recently, a more refined version of the gluino cascade analysis has been performed by D. Curtin [50], confirming this conclusion for the sbottom mass. (Note that the benchmark point used in this studies has precisely the sort of spectrum favored by current LHC constraints and naturalness, with only third-generation squarks appearing below 1 TeV.) Thus, it appears that the LHC can do a decent job on measuring the masses, at least as long as substantial samples of stops and sbottoms are produced, either directly or in cascade decays. However, as already emphasized in the discussion of radiative corrections above, the sum rule involves a delicate cancellation among the stop and sbottom terms, and even fractionally small corrections to each term can result in significant fractional corrections in Υ. It is absolutely crucial to measure the stop and sbottom masses *as precisely as possible*. An e^+e^- collider, with sufficiently high center-of-mass energy to pair-produce the stops, would be an ideal instrument for this task.

While a lot of work has been done on superpartner mass measurements, measuring mixing angles has not attracted the same attention. There are several proposals in the literature for measuring the stop mixing angle [68, 85, 91, 89]. For example, [85] proposed using the polarization of the top quarks produced in the direct decay $\tilde{t} \to t\tilde{\chi}_1^0$ as a handle on the mixing angle at the LHC; however, the measurement is quite challenging

experimentally, and even if it could be done, additional information on the neutralino composition (bino, wino and higgsino fractions) would be required for this approach to succeed. There are, to our knowledge, no proposals for measuring the sbottom mixing angle at the LHC. Unless a way to do it is found, no test of the sum rule is possible at the LHC. An e^+e^- collider, on the other hand, is ideally suited for measuring mixing angles. Stops and sbottoms are produced in e^+e^- collisions via photon or Z exchange. Since the Z couples with different strengths to left- and right-handed squarks, the Z couplings to the physical squark states (mass eigenstates) depend explicitly on the mixing angles. For example, the coupling $Z\tilde{t}_1^*\tilde{t}_1$ has the form

$$\mathcal{L} \supset -ie\left[\left(\frac{1}{6}t_w - \frac{1}{2}t_w^{-1}\right)\cos^2\theta_{\tilde{t}} + \frac{2}{3}t_w \sin^2\theta_{\tilde{t}}\right]\tilde{t}_1^*\partial_\mu\tilde{t}_1 Z^\mu, \tag{4.5}$$

where $t_w \equiv \tan\theta_w$. A measurement of the total stop or sbottom pair-production cross section gives a direct measurement of the mixing angles. This technique was explored in [19], where it was found that a rather precise determination of the stop mixing angle (fractional error of about 10% on $\cos\theta_{\tilde{t}}$) was possible at a 500 GeV e^+e^- collider. Beam polarization was found to play a crucial role in this measurement. This conclusion seem rather robust, and should be valid as long as the center-of-mass energy is high enough to produce $\tilde{t}_1$ pairs.

4.1.5 Conclusions

In this section, we described the SUSY-Yukawa sum rule, a simple prediction of SUSY which follows directly from the crucial coupling relation responsible for canceling the quadratic divergence in the Higgs mass. The sum rule involves only directly observable quantities, *i.e.* masses and mixing angles of third-generation squarks. Radiative corrections to the sum rule depend on a number of other SUSY parameters. We showed

how measuring those parameters at the LHC and the ILC can lead to a sharper theoretical prediction of the sum rule. We also discussed the prospects of measuring the third-generation squark masses and mixing angles experimentally. While the LHC can measure masses, the precision seems insufficient for a meaningful test of the sum rule. Moreover, mixing angle measurements at the LHC appear very difficult or impossible. An e^+e^- collider such as the ILC can provide precise mass and mixing angle measurements, as long as the center-of-mass energy is sufficiently high to produce both stop and sbottom states. If SUSY-like new physics is found at the LHC, this set of measurements could form an important part of the physics case for the ILC or a higher-energy e^+e^- collider.

CHAPTER 5

CONCLUSION

At the time of this writing, humanity sits at the interbellum between two LHC runs. Having finished its first run at $\sqrt{s} = 7$ and 8 TeV in 2012, the LHC will soon restart proton-proton collisions at $\sqrt{s} = 13$ TeV, and a new flurry of recasting, interpretation, and speculation will begin. We have been climbing this mountain for many years, but we are nearing the top of the crest, and we will soon be able to see what is on the other side. Will we find our lost SUSY particles, or perhaps evidence of another theory beyond the Standard Model? Or will we peek over the crest to find nothing but a desert above the weak scale?

This dissertation likely represents my final contribution to humanity's search for an explanation for the structure of the universe. But I feel extremely blessed to have contributed at all, and to have spent the last ten years in the company of fellow searchers, because these experiences have given me the deepest possible understanding of what and where we are.

APPENDIX A

APPENDIX TO SECTION 3.1: DETAILS OF THE RECASTING PROCEDURE

To recast the CMS SSDL+MET+b analysis in terms of the RPV SUSY model, we follow closely the instructions provided by CMS in [44] and its predecessors [41, 46]. The only significant difference is in the treatment of leptons. The instructions recommend analyzing leptons at parton level, by taking the leptons that pass the kinematic cuts and applying the selection efficiencies given in Section 7 of [44]. These selection efficiencies, which account for lepton identification efficiencies, isolation cuts, and detector effects, had been computed from Monte Carlo studies of simplified model A1 ($pp \to \tilde{g}\tilde{g}$, $\tilde{g} \to t\bar{t}\tilde{\chi}^0$) at the RPC SUSY benchmark point LM9. However, because the leptons in the RPV SUSY signal process may come from boosted tops, there is extra hadronic activity near the leptons, and the LM9 selection efficiencies do not properly model the isolation cuts for the RPV signal. Therefore, we extract the isolation cut efficiencies for RPV from our signal MC. To do so, we impose a lepton isolation cut on the *hadronized* signal MC events. Following [41], $Iso(\hat{\ell})$ is defined as a scalar sum of the lepton p_T's and photon and hadron E_T's within a cone of size $\Delta R \equiv \sqrt{(\Delta\eta)^2 + (\Delta\phi)^2} < 0.3$ about the lepton, not including the p_T of the lepton itself:

$$Iso(\hat{\ell}) \equiv \frac{\sum_{\Delta R<0.3} p_T(\ell \neq \hat{\ell}) + \sum_{\Delta R<0.3} E_T(\gamma) + \sum_{\Delta R<0.3} E_T(h)}{p_T(\hat{\ell})}. \tag{A.1}$$

To pass the isolation cut, the lepton must have have $Iso(\hat{\ell}) < 0.1$. On top of the isolation cut, we impose the identification efficiency, which we assume to be independent of p_T, η, and the physical process: 73% for electrons and 84% for muons. The identification efficiency for each lepton species is extracted by simulating the A1 LM9 benchmark model at hadron level, computing the lepton isolation cut efficiency Eff(Iso) for this sample using Eq. (A.1), and dividing the total selection efficiency reported by CMS by Eff(Iso).

The rest of the lepton analysis emulates [44] as closely as possible. From the set of selected leptons, we choose the "SSDL pair": the same-sign pair with the highest p_T and a pair invariant mass of at least 8 GeV. We then apply the dilepton trigger efficiency: 96% for ee, 93% for $e\mu$, and 88% for $\mu\mu$. We veto events where a third lepton (with $p_T > 10$ GeV, the normal $|\eta|$ cuts, and $Iso(l_3) < 0.2$) forms an opposite-sign same-flavor pair with one of the SSDL pair leptons, with a pair invariant mass between 76 and 106 GeV. We also veto events where a third lepton (with $p_T > 5$ GeV, the normal $|\eta|$ cuts, and $Iso(l_3) < 0.2$) forms an opposite-sign same-flavor pair with one of the SSDL pair leptons, with a pair invariant mass below 12 GeV.

The remaining physics objects are handled at parton level, following the instructions. The number of jets is a count of colored partons passing the kinematic cuts: $p_T > 40$ GeV and $|\eta| < 2.4$. To count b-tagged jets, we apply a p_T-dependent tagging efficiency, parameterized in Section 7 of [44], to all the b quarks that pass the jet kinematic cuts. To implement the cuts on H_T and $\not{E}_T$, we compute "generator-level" quantities gen-H_T and gen-$\not{E}_T$, and use the turn-on efficiency curves parameterized in Section 7 of [41] to get efficiencies for the cuts. gen-H_T is the scalar sum of p_T's of the jets that pass the kinematic cuts, and gen-$\not{E}_T$ is the magnitude of the vector sum of the $\vec{p}_T$'s of non-interacting final-state particles.

APPENDIX B

APPENDIX TO SECTION 4.1: DETAILS ON THE PMSSM AND THE CONSTRAINTS USED IN OUR SCANS

Our objective is to obtain an accurate distribution of Υ values from the allowed regions of the MSSM parameter space, given measurements at the LHC or ILC that indicate (with some uncertainty) that the universe sits at a certain benchmark point in the parameter space. In our case, we use the mSUGRA benchmark point LCC1, which has the parameters listed in Table B.1.

m_0	100 GeV
$m_{1/2}$	250 GeV
$\tan\beta$	10
A_0	-100 GeV
$\mathrm{sgn}(\mu)$	$+$

Table B.1: mSUGRA parameters at the benchmark point LCC1 [97].

In essence, this is an exercise in Bayesian inference. A *prior* probability distribution on the parameter space, which indicates our prior knowledge of what regions are or are not allowed, is "confronted" by the data, resulting in a *posterior* probability distribution, which indicates our knowledge of what regions are allowed after that data is taken into account. (The data in this case is a set of simulated measurements, and their uncertainties, of sparticle properties at the LHC or ILC.) It is from this posterior probability distribution that we extract the Υ distribution. Useful and in-depth discussions of this methodology can be found in [6, 17]. The algorithm we use to execute this confrontation is detailed in Appendix C.

We might have liked to scan over the full 108-dimensional MSSM parameter space, if it were not so computationally prohibitive. Instead, we confine ourselves to the phenomenological MSSM (pMSSM) [54]. Parameters for which nonzero values would gen-

erally lead to large, observable CP-violating effects and flavor changing neutral currents (FCNCs) are fixed at zero, leaving a 24-dimensional pMSSM parameter space. We then further constrain our scan to a subspace of the pMSSM parameter space that is most relevant to the third-generation squark sector, leaving an 11-dimensional parameter space listed in Table B.2. All other pMSSM parameters are fixed at their values at the benchmark point.

M_1, M_2, M_3	Gaugino masses
$m_{\tilde{Q}}$, $m_{\tilde{t}_R}$, $m_{\tilde{b}_R}$	3rd generation squark masses
A_t, A_b	3rd generation trilinear couplings
M_A (pole), $\tan\beta$ (m_Z), μ	Higgs sector parameters

Table B.2: Parameters that are scanned over in the phenomenological MSSM (pMSSM).

We also set a prior probability distribution, as in [17]. Parameters that can have either sign (M_1, M_2, M_3, A_t, A_b, μ) are given a prior probability distribution $P \sim \frac{1}{\sqrt{x^2+K^2}}$, where $K = 50\,\text{GeV}$, and the rest of the parameters (which are strictly positive) are given a Jeffreys prior $P \sim \frac{1}{x}$. This penalizes large values of the parameters and prevents the MCMC scan from venturing off to infinity. These priors are implemented by transforming the parameter space: parameters that can have either sign are transformed as

$$x \to x' = \sinh^{-1}\left(\frac{x}{50\,\text{GeV}}\right), \tag{B.1}$$

and parameters that are strictly positive are transformed as

$$x \to x' = \ln\left(\frac{x}{1\,\text{GeV}}\right). \tag{B.2}$$

Another advantage of these transformations is that the parameters are now dimensionless. Finally, we set the hard boundaries on the parameter space shown in Table B.3.

Finally, we must consider what data is used to confront the prior PDF and generate the posterior PDF. During the scan, points in the parameter space are assessed by the

parameters	minimum	maximum
M_1, M_2, M_3	-4 TeV	4 TeV
$m_{\tilde{Q}}$, $m_{\tilde{t}_R}$, $m_{\tilde{b}_R}$	100 GeV	4 TeV
A_t, A_b	-8 TeV	8 TeV
m_A (pole)	100 GeV	1 TeV
$\tan\beta(m_Z)$	2	60
μ	-1 TeV	1 TeV

Table B.3: Bounds on the parameter space scan.

likelihood $\mathcal{L}$ that they can generate the measured values of SUSY parameters. (See Appendix C for details on how this is done.) First, the likelihood is automatically set to zero if the SUSY spectrum of the point does not meet the following criteria:

- a neutralino LSP,
- due to LEP constraints, no new charged particles with mass below 100 GeV,
- the lightest CP-even Higgs mass is above 108 GeV (at the time of writing, the Higgs boson had not yet been discovered).

If the point passes all three criteria, then its likelihood is evaluated as the product of Gaussian likelihoods,

$$\mathcal{L}(\{x_i\}) = \prod_i \exp\left[-\frac{(x_i - \overline{x}_i)^2}{2\sigma_i^2}\right], \tag{B.3}$$

where each Gaussian corresponds to a different constraint x_i, with measured value $\overline{x}_i$ and uncertainty σ_i. Basic constraints used for all of the scans is listed in Table B.4. For the scans with simulated LHC and ILC data, additional constraints are listed in Table B.5.

constraint	$\overline{x}_i$	σ_i
m_W	80.480 GeV	0.025 GeV
$g_\mu - 2$	2.78×10^{-9}	6.0×10^{-10}
Br($b \to s\gamma$)	2.635×10^{-4}	0.256×10^{-4}

Table B.4: Basic constraints used for all the scans. Values $\overline{x}_i$ are taken from the SuSpect output spectrum for the benchmark point LCC1. Uncertainties σ_i for m_W and $g_\mu - 2$ are taken from [79], and the uncertainty for Br($b \to s\gamma$) is taken from [15].

constraint	$\overline{x}_i$	σ_i (LHC-14)	σ_i (ILC-500)
$m(\tilde{\chi}_1^0)$	97.22	4.8	0.05
$m(\tilde{\chi}_2^0) - m(\tilde{\chi}_1^0)$	82.99	1.2	0.07
$m(\tilde{\chi}_3^0) - m(\tilde{\chi}_1^0)$	260.00		4.0
$m(\tilde{\chi}_4^0) - m(\tilde{\chi}_1^0)$	279.47	2.2	2.2
$m(\tilde{\chi}_1^+)$	179.57		0.55
$m(\tilde{e}_R)$	142.82		0.05
$m(\tilde{e}_R) - m(\tilde{\chi}_1^0)$	45.6	1.0	0.2
$m(\tilde{\mu}_R) - m(\tilde{\chi}_1^0)$	45.6	1.0	0.2
$m(\tilde{\tau}_1) - m(\tilde{\chi}_1^0)$	36.2	5.0	0.3
$m(\tilde{e}_L) - m(\tilde{\chi}_1^0)$	103.5	1.2	0.2
$m(\tilde{\mu}_L) - m(\tilde{\chi}_1^0)$	103.5	1.2	1.0
$m(\tilde{\tau}_2) - m(\tilde{\chi}_1^0)$	107.5		1.1
$m(\tilde{\nu}_{eL})$	184.8		1.2
$m(h)$	109.74	0.25	0.05
$m(A)$	393.59	*	†
$m(\tilde{u}_R)$	545.1	19.0	16.0
$m(\tilde{s}_R)$	544.8	19.0	16.0
$m(\tilde{u}_L)$	561.5	17.4	9.8
$m(\tilde{s}_L)$	567.0	17.4	9.8
$m(\tilde{b}_1)$	516.5		
$m(\tilde{b}_2)$	545.4		
$m(\tilde{t}_1)$	399.2		
$m(\tilde{g})$	605.3	8.0	6.5

* require either $m(A) > 200$ or $\tan\beta < \frac{7}{200} m(A)$

† require $m(A) > 240$

Table B.5: Additional constraints used for the LHC and ILC scans. All masses are in GeV. If no uncertainty is listed, that particular constraint is not used for that scan. Values $\overline{x}_i$ are taken from the SuSpect output spectrum for the benchmark point LCC1. Uncertainties are taken from Table 2 of [17], which reproduces data from [97].

APPENDIX C

APPENDIX TO SECTION 4.1: DETAILS ON THE MARKOV CHAIN MONTE CARLO ALGORITHM

To scan the parameter space, we use a Markov Chain Monte Carlo (MCMC) algorithm in order to achieve an exploration of the allowed regions of the parameter space, with fine enough resolution, in a reasonable amount of time on a standard laptop computer. More specifically, we use an adaptive Metropolis-Hastings algorithm with simulated annealing, where a Gaussian proposal is used to choose the trial shift. The algorithm is adaptive in that the size of the trial shift in any direction in parameter space is based on the covariance matrix of the set of the Markov chains' last points, which is a measure of how large the posterior probability distribution seems to be at that time. This covariance matrix is continuously updated at every step. This technique is based on Appendix A of [17], and the description below closely follows it. Figure C.1 shows a simple example of the algorithm at work.

The standard Metropolis-Hastings algorithm

The Metropolis-Hastings algorithm explores a parameter space with a Markov chain, which is a sequence of points where each point is generated by a process that only depends on the previous point in the chain. Consider a Markov chain, with its last point $\vec{p}$ in our D-dimensional pMSSM parameter space. To produce the next point in the chain, propose a new point $\vec{q}$ by sampling a given probability density $P(\vec{q}|\vec{p})$. We can then evaluate the fitness of this point by a given Likelihood function $\mathcal{L}$ which depends on our constraints:

- If $\mathcal{L}(\vec{q}) \geq \mathcal{L}(\vec{p})$, then we accept the proposed point into the chain and set $\vec{p}' = \vec{q}$.

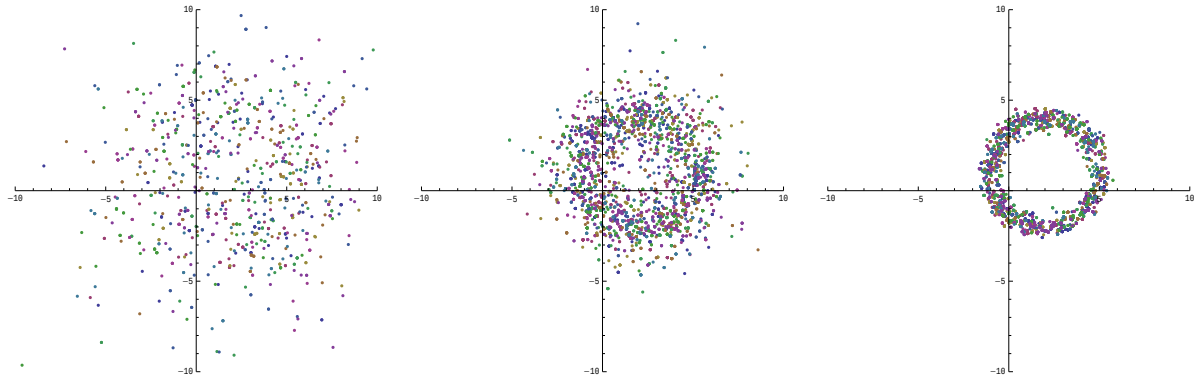

(a) (b) (c)

Figure C.1: Simple example of our Markov Chain Monte Carlo algorithm at work. 10 Markov chains are propagated for approximately 1000 steps each, constrained to seek out the region of a 2-dimensional parameter space that is a radius of 3 ± 0.3 away from the point $(2, 1)$. The plots show (a) the first 100 points of each chain, (b) points 101 to 500 of each chain, and (c) points 501 to 1000 of each chain.

- If $\mathcal{L}(\vec{q}) < \mathcal{L}(\vec{p})$, then we may still accept the proposed point and set $\vec{p}\,' = \vec{q}$, but only with probability $\frac{\mathcal{L}(\vec{q})}{\mathcal{L}(\vec{p})}$. Otherwise, we reject the proposed point and set $\vec{p}\,' = \vec{p}$.

We repeat this process, extending the Markov chain, until satisfied. This process satisfies detailed balance as long as the proposal probability density $P(\vec{q}|\vec{p})$ is symmetric with respect to $\vec{q} \leftrightarrow \vec{p}$, so the distribution of points in the Markov chain will eventually converge to the posterior probability distribution function (PDF), independent of what P actually is.

A natural choice would be to let P be a fixed Gaussian distribution centered at $\vec{p}$. Proposals are drawn randomly from a fixed neighborhood of the last point in the chain. But this would mean that the effective "step size" of each proposed shift from the last point to the new point would be fixed, whereas we may discover, over the course of the scan, that the posterior PDF is much narrower or wider in some direction in space than we had assumed. If the posterior PDF is much narrower in some direction than our guessed step size, many proposed points will be rejected. If the posterior PDF is much wider,

it will take much longer to cover the allowed parameter space. Therefore, we instead choose a more efficient Gaussian proposal that adapts to the currently-known size of the posterior PDF.

The adaptive Metropolis-Hastings algorithm

Instead of using a single Markov chain, we now use N Markov chains. Remember that to satisfy the Markov property, we can only use the set of N last points of the chains, $\{\vec{p}_i\}$, to define the proposal distribution P. Let us first construct the mean and covariance matrix of these points:

$$\vec{\mu} \equiv \frac{1}{N}\sum_{i=1}^{N}\vec{p}_i \tag{C.1}$$

$$\mathbf{C} \equiv \frac{1}{N}\sum_{i=1}^{N}(\vec{p}_i - \vec{\mu})(\vec{p}_i - \vec{\mu})^T. \tag{C.2}$$

The covariance matrix captures the size and shape of the posterior PDF at that time. (Although it is important to note that we must have $N > D$, that is, more Markov chains than dimensions in the parameter space, in order for $\mathbf{C}$ to be positive definite.)

At each step in the scan, we choose one of the Markov chains at random and update it with a new point. Let us define the "trial shift" from the last point in the chain to the proposed new point as $\vec{y} \equiv \vec{q} - \vec{p}_i$. Then, the trial shift is chosen from a Gaussian proposal distribution

$$P(\vec{y}|\mathbf{C}) = \frac{1}{\sqrt{(2\pi f^2)^D \det \mathbf{C}}}\ \exp\left(-\frac{1}{2f^2}\vec{y}^T\mathbf{C}^{-1}\vec{y}\right), \tag{C.3}$$

where $f \equiv 2.381/\sqrt{D}$ yields efficient step sizes. Computationally, the easiest way to implement this is to sample a random vector $\vec{x}$ from a D-dimensional Gaussian distribution with zero mean and unit variance in each parameter, and then setting $\vec{y} = f\mathbf{L}\vec{x}$. Here, $\mathbf{L}$ is the Cholesky decomposition of $\mathbf{C}$, which is akin to a matrix square root, and can be

readily computed by most computer linear algebra packages such as that found in the GNU Scientific Library.

We must also modify how we decide whether or not to accept the proposed shift. Since the covariance matrix $\mathbf{C}$ will be updated to a new covariance matrix $\mathbf{C}'$ if we accept the shift, the proposal distribution is no longer symmetric, and using the old method of deciding whether to accept the shift would result in a loss of detailed balance. We can recover detailed balance by making our probability of accepting the proposed shift

$$P(\text{acceptance}) = \min\left[1, \frac{P(\vec{y}|\mathbf{C}')\,\mathcal{L}(\vec{q})}{P(\vec{y}|\mathbf{C})\,\mathcal{L}(\vec{p}_i)}\right]. \tag{C.4}$$

For the above computation, it is necessary to get the new values of the covariance matrix, its determinant, and its inverse. But recalculating these quantities is the most computationally intensive part of the entire algorithm, if the number of dimensions (and thus the number of chains) is large. Instead, we use a shortcut that allows us to only invert the covariance matrix once, at the start. The mean and covariance matrix are updated with

$$\vec{\mu}\,' = \vec{\mu} + \frac{1}{N}\vec{y}, \tag{C.5}$$

$$\mathbf{C}' = \mathbf{C} + \frac{1}{N}(\vec{p}_i - \vec{\mu})\vec{y}^{\,T} + \frac{1}{N}\vec{y}(\vec{p}_i - \vec{\mu})^T + \frac{N-1}{N^2}\vec{y}\vec{y}^{\,T}, \tag{C.6}$$

where the ith Markov chain is being updated. Casting the update of the covariance matrix in terms of dyad products allows us to calculate the determinant and inverse easily. If we write

$$\mathbf{C}' = \mathbf{C} + \sum_i \vec{a}_i \vec{b}_i{}^T, \tag{C.7}$$

then we can simply use

$$\begin{aligned} \lambda_{ij} &= \vec{b}_i{}^T \mathbf{C}^{-1} \vec{a}_j, \\ \mathbf{C}'^{-1} &= \mathbf{C}^{-1} - \sum_{i,j} (\mathbf{1}+\lambda)^{-1}_{ij}\ \mathbf{C}^{-1}\ \vec{a}_i \vec{b}_j{}^T\ \mathbf{C}^{-1}, \\ \det \mathbf{C}' &= \det \mathbf{C}\ \det(\mathbf{1}+\lambda). \end{aligned} \tag{C.8}$$

Simulated annealing

We make one more modification to the Metropolis-Hastings algorithm: simulated annealing. We consider the first 10% of points in the scan the "burn-in period", where we make it easier for the chains to jump to points in the parameter space with lower likelihoods. In a sense, the scan starts out "hot", with the chains jumping liberally to far-flung regions in parameter space, and then it "cools down" to the normal behavior. This allows the chains to start out with a better chance of exploring multiple parts of the parameter space at once, especially if the allowed regions of parameter space happen to be disconnected. After the scan is completed, the burn-in period is removed from the chains.

To implement this, the likelihood function is modified with an exponent for the first half of the burn-in period: $\mathcal{L} \to \mathcal{L}^\lambda$ (unrelated to the λ in Eq. C.8). This exponent is defined as $\lambda = (0.01)^{1-\alpha}$, where α is the fraction of the burn-in period that has elapsed. Thus, at the start, $\lambda = 0.01$* and the effect of the likelihood ratio on the probability of accepting a new shift is lowered. But as the system cools down, $\lambda \to 0.1$ and the likelihood ratio matters more. Finally, for the last half of the burn-in period, the exponent is turned off and things proceed normally.

Convergence testing

At the end of the scan, we test for convergence following the procedure in Appendix A.4 in [17], fully derived in [58].

*That's NumberWang!

BIBLIOGRAPHY

[1] Search for Supersymmetry in final states with two same-sign leptons, jets and missing transverse momentum with the ATLAS detector in pp collisions at $\sqrt{s} = 8$ TeV. 2012.

[2] Georges Aad et al. ATLAS measurements of the properties of jets for boosted particle searches. *Phys.Rev.*, D86:072006, 2012, 1206.5369.

[3] Georges Aad et al. Search for pair production of massive particles decaying into three quarks with the ATLAS detector in $\sqrt{s} = 7$ TeV pp collisions at the LHC. *JHEP*, 1212:086, 2012, 1210.4813.

[4] Georges Aad et al. Search for squarks and gluinos using final states with jets and missing transverse momentum with the ATLAS detector in $\sqrt{s} = 7$ TeV proton-proton collisions. *Phys.Lett.*, B710:67–85, 2012, 1109.6572.

[5] A. Abdesselam, E. Bergeaas Kuutmann, U. Bitenc, G. Brooijmans, J. Butterworth, et al. Boosted objects: A Probe of beyond the Standard Model physics. *Eur.Phys.J.*, C71:1661, 2011, 1012.5412.

[6] Shehu S. AbdusSalam, Benjamin C. Allanach, Fernando Quevedo, Farhan Feroz, and Mike Hobson. Fitting the Phenomenological MSSM. *Phys.Rev.*, D81:095012, 2010, 0904.2548.

[7] T. Abe et al. Linear Collider Physics Resource Book for Snowmass 2001 - Part 2: Higgs and Supersymmetry Studies. 2001, hep-ex/0106056.

[8] Bobby Samir Acharya, Phill Grajek, Gordon L. Kane, Eric Kuflik, Kerim Suruliz, et al. Identifying Multi-Top Events from Gluino Decay at the LHC. 2009, 0901.3367.

[9] Kaustubh Agashe, Alexander Belyaev, Tadas Krupovnickas, Gilad Perez, and Joseph Virzi. LHC Signals from Warped Extra Dimensions. *Phys.Rev.*, D77:015003, 2008, hep-ph/0612015.

[10] B.C. Allanach and Ben Gripaios. Hide and Seek With Natural Supersymmetry at the LHC. *JHEP*, 1205:062, 2012, 1202.6616.

[11] A. Altheimer, S. Arora, L. Asquith, G. Brooijmans, J. Butterworth, et al. Jet Substructure at the Tevatron and LHC: New results, new tools, new benchmarks. *J.Phys.*, G39:063001, 2012, 1201.0008.

[12] Daniele Alves et al. Simplified Models for LHC New Physics Searches. *J.Phys.*, G39:105005, 2012, 1105.2838.

[13] Johan Alwall, Michel Herquet, Fabio Maltoni, Olivier Mattelaer, and Tim Stelzer. MadGraph 5 : Going Beyond. *JHEP*, 1106:128, 2011, 1106.0522.

[14] Masaki Asano, Krzysztof Rolbiecki, and Kazuki Sakurai. Can R-parity violation hide vanilla supersymmetry at the LHC? *JHEP*, 1301:128, 2013, 1209.5778.

[15] D. Asner et al. Averages of b-hadron, c-hadron, and τ-lepton properties. 2010, 1010.1589.

[16] Yang Bai, Andrey Katz, and Brock Tweedie. Pulling Out All the Stops: Searching for RPV SUSY with Stop-Jets. *JHEP*, 1401:040, 2014, 1309.6631.

[17] Edward A. Baltz, Marco Battaglia, Michael E. Peskin, and Tommer Wizansky. Determination of dark matter properties at high-energy colliders. *Phys.Rev.*, D74:103521, 2006, hep-ph/0602187.

[18] Priyotosh Bandyopadhyay and Biplob Bhattacherjee. Boosted top quarks in supersymmetric cascade decays at the LHC. *Phys.Rev.*, D84:035020, 2011, 1012.5289. (Signal rates for a SUSY search, in the context of constrained MSSM, using a single top tag were computed here. However, this paper did not analyze the backgrounds, which are quite strong in this channel.).

[19] A. Bartl, H. Eberl, S. Kraml, W. Majerotto, W. Porod, et al. Search of stop, sbottom, tau sneutrino, and stau at an e+ e- linear collider with S**(1/2) = 0.5-TeV - 2-TeV. *Z.Phys.*, C76:549–560, 1997, hep-ph/9701336.

[20] Valeria Bartsch and Gunter Quast. Expected Signal Observability at Future Experiments. 2005.

[21] G.L. Bayatian et al. CMS technical design report, volume II: Physics performance. *J.Phys.*, G34:995–1579, 2007.

[22] W. Beenakker, R. Hopker, and M. Spira. PROSPINO: A Program for the production of supersymmetric particles in next-to-leading order QCD. 1996, hep-ph/9611232.

[23] Joshua Berger, Csaba Csaki, Yuval Grossman, and Ben Heidenreich. Mesino Oscillation in MFV SUSY. *Eur.Phys.J.*, C73:2408, 2013, 1209.4645.

[24] Joshua Berger, Maxim Perelstein, Michael Saelim, and Andrew Spray. Boosted Tops from Gluino Decays. 2011, 1111.6594.

[25] Joshua Berger, Maxim Perelstein, Michael Saelim, and Philip Tanedo. The Same-Sign Dilepton Signature of RPV/MFV SUSY. *JHEP*, 1304:077, 2013, 1302.2146.

[26] G. Bevilacqua, M. Czakon, C.G. Papadopoulos, and M. Worek. Dominant QCD Backgrounds in Higgs Boson Analyses at the LHC: A Study of pp $\rightarrow$ t anti-t + 2 jets at Next-To-Leading Order. *Phys.Rev.Lett.*, 104:162002, 2010, 1002.4009. G. Bevilacqua, M. Czakon, C.G. Papadopoulos, and M. Worek. Hadronic top-quark pair production in association with two jets at Next-to-Leading Order QCD. *Phys.Rev.*, D84:114017, 2011, 1108.2851.

[27] Biplob Bhattacherjee, Jason L. Evans, Masahiro Ibe, Shigeki Matsumoto, and Tsutomu T. Yanagida. Natural supersymmetrys last hope: R-parity violation via UDD operators. *Phys.Rev.*, D87(11):115002, 2013, 1301.2336.

[28] Monika Blanke, David Curtin, and Maxim Perelstein. SUSY-Yukawa Sum Rule at the LHC. *Phys.Rev.*, D82:035020, 2010, 1004.5350.

[29] Joseph Bramante, Jason Kumar, and Brooks Thomas. Large Jet Multiplicities and New Physics at the LHC. *Phys.Rev.*, D86:015014, 2012, 1109.6014.

[30] Christopher Brust, Andrey Katz, Scott Lawrence, and Raman Sundrum. SUSY, the Third Generation and the LHC. *JHEP*, 1203:103, 2012, 1110.6670.

[31] Christopher Brust, Andrey Katz, and Raman Sundrum. SUSY Stops at a Bump. *JHEP*, 1208:059, 2012, 1206.2353.

[32] Michael Burns, Kyoungchul Kong, Konstantin T. Matchev, and Myeonghun Park. Using Subsystem MT2 for Complete Mass Determinations in Decay Chains with Missing Energy at Hadron Colliders. *JHEP*, 0903:143, 2009, 0810.5576.

[33] Jonathan M. Butterworth, Adam R. Davison, Mathieu Rubin, and Gavin P. Salam. Jet substructure as a new Higgs search channel at the LHC. *Phys.Rev.Lett.*, 100:242001, 2008, 0802.2470.

[34] Matteo Cacciari and Gavin P. Salam. Dispelling the N^3 myth for the k_t jet-finder. *Phys.Lett.*, B641:57–61, 2006, hep-ph/0512210.

[35] Matteo Cacciari, Gavin P. Salam, and Gregory Soyez. Fastjet. http://fastjet.fr.

[36] Matteo Cacciari, Gavin P. Salam, and Gregory Soyez. FastJet User Manual. *Eur.Phys.J.*, C72:1896, 2012, 1111.6097.

[37] John M. Campbell and R. Keith Ellis. $t\bar{t}W^{+-}$ production and decay at NLO. *JHEP*, 1207:052, 2012, 1204.5678.

[38] Spencer Chang, Can Kilic, and Takemichi Okui. Measuring Top Squark Interactions With The Standard Model Through Associated Production. *Phys.Rev.*, D84:035015, 2011, 1105.1332.

[39] Serguei Chatrchyan et al. Search for Supersymmetry at the LHC in Events with Jets and Missing Transverse Energy. *Phys.Rev.Lett.*, 107:221804, 2011, 1109.2352.

[40] Serguei Chatrchyan et al. Search for anomalous t t-bar production in the highly-boosted all-hadronic final state. *JHEP*, 1209:029, 2012, 1204.2488.

[41] Serguei Chatrchyan et al. Search for new physics in events with same-sign dileptons and b-tagged jets in pp collisions at $\sqrt{s} = 7$ TeV. *JHEP*, 1208:110, 2012, 1205.3933.

[42] Serguei Chatrchyan et al. Search for three-jet resonances in pp collisions at $\sqrt{s} = 7$ TeV. *Phys.Lett.*, B718:329–347, 2012, 1208.2931.

[43] Serguei Chatrchyan et al. Identification of b-quark jets with the CMS experiment. *JINST*, 8:P04013, 2013, 1211.4462.

[44] Serguei Chatrchyan et al. Search for new physics in events with same-sign dileptons and b jets in pp collisions at $\sqrt{s} = 8$ TeV. *JHEP*, 1303:037, 2013, 1212.6194.

[45] Timothy Cohen, Eder Izaguirre, Mariangela Lisanti, and Hou Keong Lou. Jet Substructure by Accident. *JHEP*, 1303:161, 2013, 1212.1456.

[46] CMS Collaboration. Search for supersymmetry in events with same-sign dileptons. 2012.

[47] CMS Collaboration. Search for new physics in events with same-sign dileptons and jets in pp collisions at 8 TeV. 2013.

[48] Csaba Csaki, Yuval Grossman, and Ben Heidenreich. MFV SUSY: A Natural Theory for R-Parity Violation. *Phys.Rev.*, D85:095009, 2012, 1111.1239.

[49] Csaba Csaki and Ben Heidenreich. A Complete Model for R-parity Violation. *Phys.Rev.*, D88:055023, 2013, 1302.0004.

[50] David Curtin. Mixing It Up With MT2: Unbiased Mass Measurements at Hadron Colliders. *Phys.Rev.*, D85:075004, 2012, 1112.1095.

[51] J. de Favereau et al. DELPHES 3, A modular framework for fast simulation of a generic collider experiment. *JHEP*, 1402:057, 2014, 1307.6346.

[52] Nishita Desai and Biswarup Mukhopadhyaya. R-parity violating resonant stop production at the Large Hadron Collider. *JHEP*, 1010:060, 2010, 1002.2339.

[53] Nishita Desai and Biswarup Mukhopadhyaya. Constraints on supersymmetry with light third family from LHC data. *JHEP*, 1205:057, 2012, 1111.2830.

[54] A. Djouadi et al. The Minimal supersymmetric standard model: Group summary report. 1998, hep-ph/9901246.

[55] Abdelhak Djouadi, Jean-Loic Kneur, and Gilbert Moultaka. SuSpect: A Fortran code for the supersymmetric and Higgs particle spectrum in the MSSM. *Comput.Phys.Commun.*, 176:426–455, 2007, hep-ph/0211331.

[56] H.K. Dreiner and T. Stefaniak. Bounds on R-parity Violation from Resonant Slepton Production at the LHC. *Phys.Rev.*, D86:055010, 2012, 1201.5014.

[57] Daniel Duggan, Jared A. Evans, James Hirschauer, Ketino Kaadze, David Kolchmeyer, et al. Sensitivity of an Upgraded LHC to R-Parity Violating Signatures of the MSSM. 2013, 1308.3903.

[58] Joanna Dunkley, Martin Bucher, Pedro G. Ferreira, Kavilan Moodley, and Constantinos Skordis. Fast and reliable mcmc for cosmological parameter estimation. *Mon.Not.Roy.Astron.Soc.*, 356:925–936, 2005, astro-ph/0405462.

[59] Gauthier Durieux and Christopher Smith. The same-sign top signature of R-parity violation. *JHEP*, 1310:068, 2013, 1307.1355.

[60] Rouven Essig, Eder Izaguirre, Jared Kaplan, and Jay G. Wacker. Heavy Flavor Simplified Models at the LHC. *JHEP*, 1201:074, 2012, 1110.6443.

[61] Jared A. Evans and Yevgeny Kats. LHC Coverage of RPV MSSM with Light Stops. *JHEP*, 1304:028, 2013, 1209.0764.

[62] Gary J. Feldman and Robert D. Cousins. A Unified approach to the classical statistical analysis of small signals. *Phys.Rev.*, D57:3873–3889, 1998, physics/9711021.

[63] R. Franceschini and R.N. Mohapatra. New Patterns of Natural R-Parity Violation with Supersymmetric Gauged Flavor. *JHEP*, 1304:098, 2013, 1301.3637.

[64] Roberto Franceschini and Riccardo Torre. RPV stops bump off the background. *Eur.Phys.J.*, C73:2422, 2013, 1212.3622.

[65] Tony Gherghetta and Alex Pomarol. The Standard model partly supersymmetric. *Phys.Rev.*, D67:085018, 2003, hep-ph/0302001.

[66] Tony Gherghetta, Benedict von Harling, and Nicholas Setzer. A natural little hierarchy for RS from accidental SUSY. *JHEP*, 1107:011, 2011, 1104.3171.

[67] Zhenyu Han, Andrey Katz, Minho Son, and Brock Tweedie. Boosting Searches for Natural SUSY with RPV via Gluino Cascades. *Phys.Rev.*, D87:075003, 2013, 1211.4025.

[68] Junji Hisano, Kiyotomo Kawagoe, and Mihoko M. Nojiri. A Detailed study of the gluino decay into the third generation squarks at the CERN LHC. *Phys.Rev.*, D68:035007, 2003, hep-ph/0304214.

[69] Anson Hook, Eder Izaguirre, Mariangela Lisanti, and Jay G. Wacker. High Multiplicity Searches at the LHC Using Jet Masses. *Phys.Rev.*, D85:055029, 2012, 1202.0558.

[70] H. Ita, Z. Bern, L.J. Dixon, Fernando Febres Cordero, D.A. Kosower, et al. Precise Predictions for Z + 4 Jets at Hadron Colliders. *Phys.Rev.*, D85:031501, 2012, 1108.2229.

[71] Thomas Junk. Confidence level computation for combining searches with small statistics. *Nucl.Instrum.Meth.*, A434:435–443, 1999, hep-ex/9902006.

[72] Gordon L. Kane, Eric Kuflik, Ran Lu, and Lian-Tao Wang. Top Channel for Early SUSY Discovery at the LHC. *Phys.Rev.*, D84:095004, 2011, 1101.1963.

[73] David E. Kaplan, Keith Rehermann, Matthew D. Schwartz, and Brock Tweedie. Top Tagging: A Method for Identifying Boosted Hadronically Decaying Top Quarks. *Phys.Rev.Lett.*, 101:142001, 2008, 0806.0848.

[74] Adam Kardos, Zoltan Trocsanyi, and Costas Papadopoulos. Top quark pair production in association with a Z-boson at NLO accuracy. *Phys.Rev.*, D85:054015, 2012, 1111.0610.

[75] Yevgeny Kats, Patrick Meade, Matthew Reece, and David Shih. The Status of GMSB After 1/fb at the LHC. *JHEP*, 1202:115, 2012, 1110.6444.

[76] Can Kilic and Scott Thomas. Signatures of Resonant Super-Partner Production with Charged-Current Decays. *Phys.Rev.*, D84:055012, 2011, 1104.1002.

[77] Gordan Krnjaic and Daniel Stolarski. Gauging the Way to MFV. *JHEP*, 1304:064, 2013, 1212.4860.

[78] Ben Lillie, Lisa Randall, and Lian-Tao Wang. The Bulk RS KK-gluon at the LHC. *JHEP*, 0709:074, 2007, hep-ph/0701166.

[79] K. Nakamura et al. Review of particle physics. *J.Phys.*, G37:075021, 2010.

[80] Emanuel Nikolidakis and Christopher Smith. Minimal Flavor Violation, Seesaw, and R-parity. *Phys.Rev.*, D77:015021, 2008, 0710.3129.

[81] Michele Papucci, Joshua T. Ruderman, and Andreas Weiler. Natural SUSY Endures. *JHEP*, 1209:035, 2012, 1110.6926.

[82] Maxim Perelstein and Michael Saelim. SUSY-Yukawa Sum Rule at the LHC and the ILC. 2012, 1201.5839.

[83] Maxim Perelstein and Christian Spethmann. A Collider signature of the supersymmetric golden region. *JHEP*, 0704:070, 2007, hep-ph/0702038.

[84] Maxim Perelstein and Andrew Spray. Tensor Reggeons from Warped Space at the LHC. *JHEP*, 0910:096, 2009, 0907.3496. Maxim Perelstein and Andrew Spray. Four boosted tops from a Regge gluon. *JHEP*, 1109:008, 2011, 1106.2171.

[85] Maxim Perelstein and Andreas Weiler. Polarized Tops from Stop Decays at the LHC. *JHEP*, 0903:141, 2009, 0811.1024.

[86] Tilman Plehn, Gavin P. Salam, and Michael Spannowsky. Fat Jets for a Light Higgs. *Phys.Rev.Lett.*, 104:111801, 2010, 0910.5472.

[87] Tilman Plehn, Michael Spannowsky, Michihisa Takeuchi, and Dirk Zerwas. Stop Reconstruction with Tagged Tops. *JHEP*, 1010:078, 2010, 1006.2833.

[88] Alexander L. Read. Modified frequentist analysis of search results (The CL(s) method). 2000.

[89] Krzysztof Rolbiecki, Jamie Tattersall, and Gudrid Moortgat-Pick. Towards Measuring the Stop Mixing Angle at the LHC. *Eur.Phys.J.*, C71:1517, 2011, 0909.3196.

[90] Michael Saelim and Maxim Perelstein. RPV SUSY with Same-Sign Dileptons at LHC-14. 2013, 1309.7707.

[91] Jessie Shelton. Polarized tops from new physics: signals and observables. *Phys.Rev.*, D79:014032, 2009, 0811.0569.

[92] Torbjorn Sjostrand, Stephen Mrenna, and Peter Z. Skands. A Brief Introduction to PYTHIA 8.1. *Comput.Phys.Commun.*, 178:852–867, 2008, 0710.3820.

[93] Alessandro Strumia. The Fine-tuning price of the early LHC. *JHEP*, 1104:073, 2011, 1101.2195.

[94] Raman Sundrum. SUSY Splits, But Then Returns. *JHEP*, 1101:062, 2011, 0909.5430.

[95] Jesse Thaler and Ken Van Tilburg. Identifying Boosted Objects with N-subjettiness. *JHEP*, 1103:015, 2011, 1011.2268. Jesse Thaler and Ken Van Tilburg. Maximizing Boosted Top Identification by Minimizing N-subjettiness. *JHEP*, 1202:093, 2012, 1108.2701.

[96] Manuel Toharia and James D. Wells. Gluino decays with heavier scalar superpartners. *JHEP*, 0602:015, 2006, hep-ph/0503175.

[97] G. Weiglein et al. Physics interplay of the LHC and the ILC. *Phys.Rept.*, 426:47–358, 2006, hep-ph/0410364.